Fluorescent biomarkers for membrane separation

Anja Ruud Winther

The Department of Biosciences
The Faculty of Mathematics and Natural Sciences

THE UNIVERSITY OF OSLO

December 2015

Year: 2015

Title: Fluorescent Biomarkers for Membrane Separation

Anja Ruud Winther

http://www.duo.uio.no/

Print: Reprosentralen, the University of Oslo

Abstract

The verification of the protein content in membrane fractions after separation of Gram-negative bacterial membranes is to date a tedious and demanding process. With this project, we wanted to create *Escherichia coli* (*E. coli*) strains with a stable expression of membrane bound fluorescent biomarkers. Labeling the membranes of *E. coli* BL21 Gold (DE3) with fluorescent proteins allows a membrane separation to be easily verified with simple fluorescence detection. Furthermore, we wanted to investigate and compare the grade of separation obtainable with the two membrane separation techniques selective detergent treatment and density gradient centrifugation.

Six fluorescent membrane labels were produced by fusing the genes encoding a fluorescent protein and a membrane protein, or an artificial signal sequence. These fusion genes were expressed from the plasmid pACYCDuet-1 in *E. coli* BL21 Gold (DE3), and the membranes were separated with the selective detergent treatment. This method proved to be an outer membrane (OM) enrichment technique, where the OM fraction was relatively clean, while the inner membrane (IM) fraction contained contaminants in the form of OM proteins and lipopolysaccharides. Four membrane labels were chosen for further experiments based on the transport to the intended membrane and the grade of separation obtained with the selective detergent treatment. In the next part of the project, the transport and localization of the fluorescent biomarkers to the intended membrane was verified by utilizing the density gradient centrifugation technique. This proved to require more precision and time, but gave a more complete separation of the two membranes.

The biggest issue with the fluorescent biomarkers was the loss of a major part of the total fluorescence after fluorescent protein expression and separation of the membranes. We found that biologically active inclusion bodies were part of the problem, and the addition of a centrifugation step of 10 000 x *g* before pelleting the membranes removed these from the membrane fractions. To reduce the accumulation of inclusion bodies in the cells, a lower expression level of the fluorescent biomarkers was required.

In the final stage of the project, the two most suitable fluorescent markers were to be transferred into the *E. coli* BL21 Gold (DE3) genome using λ red recombination. Due to time limitations, this part of the project was not completed. More experimentation and optimization is required to obtain recombinant clones with this technique.

Acknowledgements

First of all, I want to thank my supervisors, Prof. Dirk Linke and Dr. Jack Leo for giving me the opportunity to work with this project. I have learned a lot about science, Gram-negative bacteria, and bacterial surface proteins during my time in the lab, thanks to them. I also want to thank the rest of the Dirk Linke group at the University of Oslo for support and a lot of good ideas.

Furthermore, I want to thank Vilde Olsson for gossip and encouragement during our daily 11.45 lunches throughout the four semesters I spent on my master's degree. Thank you for all the laughs we have shared and I'm sorry for all the complaints you have listened to!

To my fiancé and my maid of honour: thank you for lending shoulders to cry on, immense support, and good times. Love you!

And finally, a thank you to my mom, my dad and my sister for being an inspiration and supporting me in everything I do.

Table of contents

1 Introduction

This project came about due to the need for a simple way to verify the quality of membrane separation techniques. As Gram-negative bacteria have two membranes, it is essential to be able to confirm a membrane separation as complete, and to detect prospective contaminations between the two fractions. There are several membrane isolation and separation techniques to choose from when working with Gram-negative bacteria. The standard technique used in the Dirk Linke laboratory is an outer membrane (OM) enrichment protocol that is relatively quick and simple. This OM enrichment uses a selective detergent, lauroyl sarcosine, to solubilize the inner membrane (IM). Previous work by the group (Thein *et al.*, 2010) compares several of these membrane separation techniques, including a similar technique to the OM enrichment method. Also included in this work is a separation method that takes advantage of the different densities of the two membranes and separates them using density gradient centrifugation. This is a more extensive technique that is time consuming compared to the OM enrichment method. In the publication by Thein *et al*., 2010, various methods were used to investigate the quality of the separation techniques by looking at the protein content of the fractions. These include sodium dodecyl sulphate polyacrylamide gel electrophoresis (SDS-PAGE), immunoblotting, and mass spectrometric analysis. All of these, in particular mass spectrometric analysis, are time consuming. A quick and easy solution would be to label the two membranes with fluorescent proteins and measure the fluorescence of the fractions after separation. In this project, my aims were to (i) create such *Escherichia coli* (*E. coli*) strains with fluorescently labeled membranes, and (ii) evaluate the two membrane separation techniques mentioned above based on the ability to produce fractions purely containing the intended fluorescent protein.

1.1 Theory

1.1.1 Gram-negative bacteria

Gram-negative bacteria, such as *E. coli*, have two membranes, the IM and the OM. The space between the two membranes is called the periplasmic compartment, or the periplasm. The periplasm contains a peptidoglycan layer – a polysaccharide of the repeated disaccharide N-acetylglucosamine and N-acetylmuramic acid, with peptide side chains. The IM is composed

of phospholipid and proteins that are either integral membrane proteins or peripherally attached proteins. The same types of proteins are found in the OM. The inner leaflet of the OM of Gram-negative bacteria is composed of phospholipids while the outer leaflet is composed of lipopolysaccharides (LPS). LPS consist of three domains: lipid A or the membrane anchor, the core, and the O-antigen sidechain. LPS make a protective coat around the bacteria, protecting it from damage from its environment, such as from antibiotics. Lipid A is an important factor in *E. coli* pathogenicity. It is an endotoxin that can, in high concentrations, induce host shock due to an excessive immune response.

1.1.2 Protein transport in *Escherichia coli*

The membrane proteins of *E. coli* are integral membrane proteins and peripherally attached proteins. With proteins destined for the periplasm, the membrane proteins cross the IM through the general Secretion (Sec) translocase or the Twin Arginine (Tat) Translocase. The Sec pathway transports unfolded proteins across the IM or transfers integral membrane proteins into the IM (Sato *et al.*, 1997), while the Tat pathway transports fully folded proteins across the membrane or transfers integral membrane proteins into the IM (DeLisa *et al.*, 2003, Bachmann *et al.*, 2006).

The Sec pathway for membrane transport

The recognition of a protein destined for transport through the Sec translocase is through a hydrophobic amino terminal signal peptide, which is the first segment of the polypeptide to be translated by the ribosome. This signal peptide is made up of a hydrophobic core flanked by polar regions on either side (Heijne, 1983). The hydrophobic core adopts an α-helical secondary structure. The sequence has a conserved A-X-A motif in the carboxyl-terminal region, which is where the signal sequence is cleaved off by the leader peptidase (Lep) A after translocation (Heijne, 1983, Dalbey and Wickner, 1985). Dalbey and Wickner, 1985 showed that LepA is necessary for release of the exported protein from the IM, not for the actual transport across the membrane. Integral membrane proteins destined for the IM can therefore remain uncleaved. In this case, the hydrophobic signal peptide functions as the membrane anchor of the integral membrane protein, and is called a signal anchor.

Studies show that ribosomes can be translocated to the cytoplasmic membrane while translating proteins targeted for the Sec pathway (Walter and Blobel, 1981). This is the co-

translational mechanism, and is most common for IM integral proteins. The signal recognition particle (SRP) attaches to the ribosome, temporarily halting the translation, and docks the ribosome at the IM through its receptor FtsY (Figure 1) (Rapiejko and Gilmore, 1994). Both FtsY and the SRP have guanosine 5'-triphosphate (GTP) binding sites, and the binding of FtsY to the SRP prompts a conformational change that increases FtsY's affinity for GTP (Shan and Walter, 2003). SecY, a component in the Sec translocase complex, works as a membrane anchor for FtsY (Angelini *et al.*, 2005). When the ribosome with the polypeptide chain to be translocated is transferred to the SecYEG complex, the pore forming complex of the Sec translocase, FtsY and the SRP dissociates by hydrolyzing their bound GTP (Connolly *et al.*, 1991). Proteins destined for the periplasm or OM are recognized by chaperones, such as SecB, after translation in cytosol (Figure 1) (Baars *et al*., 2006). This is the post-translational mechanism. The chaperones keep the polypeptide from folding in the cytosol while the chain is fed through the Sec translocase with the energy from adenosine 5'–triphosphate (ATP) hydrolysis (Kumamoto and Beckwith, 1985). In both co-translational and post-translational transport, SecA feeds the polypeptide chain through the SecYEG complex with energy from cycles of ATP binding and hydrolysis (Zimmer *et al.*, 2008).

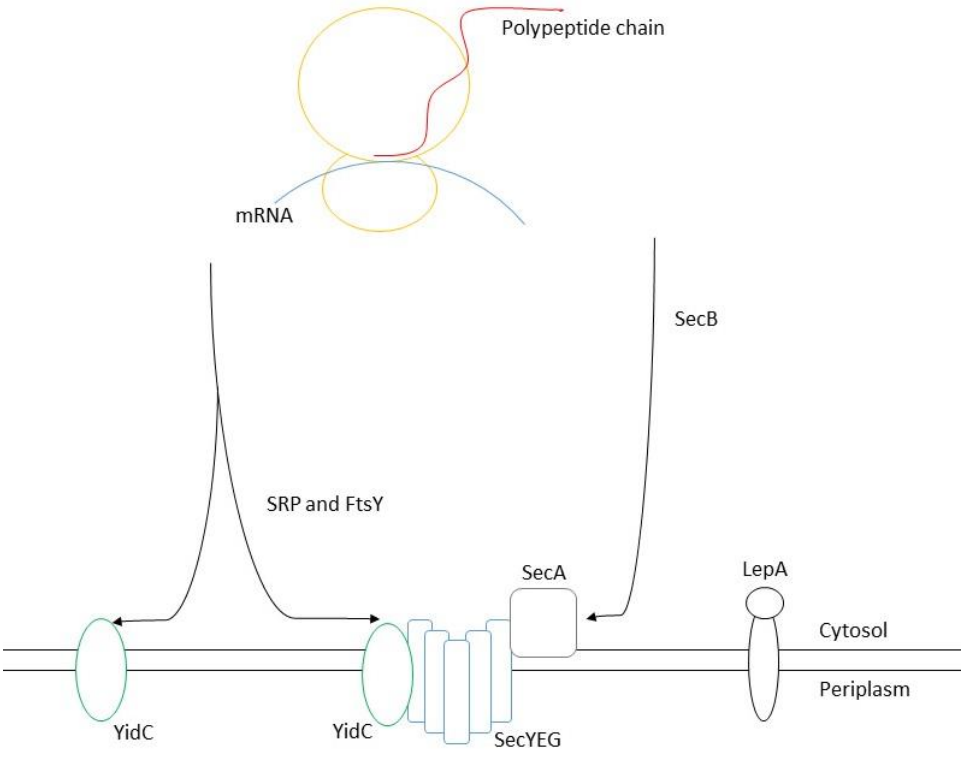

Figure 1: Simplified illustration of the Sec pathway: Translation is halted by binding by the SRP, and the protein-ribosome complex is transferred to the SecYEG complex or to the YidC insertase. This is the co-translational pathway. In the post-translational pathway, chaperones can bind the translated polypeptide chain, prevent folding, and feed the chain through SecYEG. Both pathways through the SecYEG complex require ATP hydrolysis by SecA. LepA is the peptidase that cleaves off the signal peptide after transport. This figure is modified from Du Plessis *et al.*, 2011.

Evidence of other pathways for protein transport across the IM also exists. One of these is the YidC-only pathway, which is a Sec-independent pathway (Figure 1). Even though YidC is found tightly associated with the SecYEG complex during protein transport *(*Scotti *et al.*, 2000), the insertase YidC can also insert proteins into the IM in a Sec-independent pathway. Examples of such proteins are the phage pf3 major coat protein (pf3) and the M13 phage coat protein (Serek *et al*., 2004, Klenner *et al.*, 2008). Klenner *et al.*, 2008 found that of the six transmembrane segments (TMSs) of YidC, pf3 is in direct contact with two, TMSs one and three, during membrane insertion. These two segments are part of the hydrophobic binding pocket of YidC. Proteins to be inserted into the IM by YidC first make contact with the C1 region of the insertase, and is then transferred to the hydrophobic binding pocket (Kumazaki *et al.*, 2014) (Figure 2). From here, the hydrophobic region of the substrate protein is transferred to the membrane, while the hydrophilic part that first made contact with the insertase is translocated to the periplasmic side of the membrane (Kumazaki *et al.*, 2014).

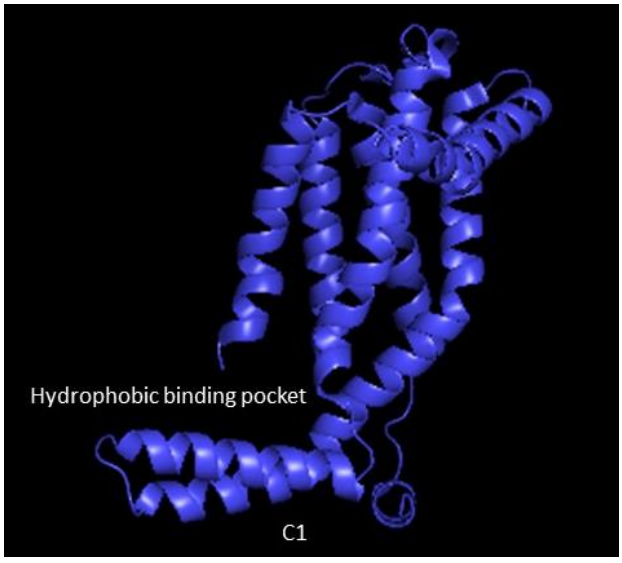

Figure 2: Crystal structure of YidC (PDB: 3WO7)

The Sec translocase

The Sec translocase forms a channel in the membrane, where the core consists of the ten TMSs of SecY. Associated with this core channel is one TMS of SecE (which has three TMSs) and the two TMSs of SecG (van den Berg *et al*., 2004). The SecYEG complex can open laterally and transfer proteins into the IM during translocation (Egea and Stroud, 2010). This transfer is initiated by a region containing a hydrophobic α-helix (Sato *et al*., 1997). The narrow part of the SecY channel is lined with hydrophobic residues and is closed by an α-helical plug. Together, the plug and the hydrophobic residues prevent leakage of ions through

the channel. During transport, constriction of the channel, the plug, and the moving polypeptide will contribute to the reduction of this ion loss (van den Berg *et al.*, 2004). SecA, the peripheral membrane ATPase associated with SecYEG, is required for protein transport through the SecYEG channel (Duong and Wickner, 1997). Associated with the SecYEG translocase is a complex consisting of SecD, SecF and YajC. Studies suggests that this complex is important for stabilizing SecA, and for the later stages of protein translocation (Duong and Wickner, 1997).

The Twin Arginine Translocase pathway for protein transport

As mentioned above, the Tat translocase transports fully folded proteins across the IM. This is necessary for proteins containing cofactors, as the cofactor is not abundant outside the cell and the protein has to "pick it up" and fold around it before being transported out of the cytoplasm (Berks, 1996). Another reason for the requirement of folding inside the cell is that the protein needs folding assistance from chaperones only found in the cytoplasm (Palmer and Berks, 2012). The signal peptide required for transport through the Tat translocase is found on the amino terminus of the protein. Berks, 1996 showed that this signal peptide is similar to the Sec signal peptide, but longer, and contains the consensus sequence S/T-R-R-X-F-L-K, where the X is a polar amino acid or glycine (G). The two arginine residues in this sequence give the Tat pathway its name, and they are completely necessary for the recognition of the signal peptide. The hydrophobic core of the Tat signal peptide is less hydrophobic compared to the signal peptide for the Sec pathway (Cristóbal *et al*., 1999).

The translocation through the Tat translocase is driven by the proton motive force (Santini *et al*., 1998). During transport, the TatBC complex first recognizes the substrate and binds it via the signal peptide, then TatA oligomerizes in the membrane to form a channel and associates with the TatBC-substrate complex (Cline and Mori, 2001) (Figure 3). TatB has one transmembrane α-helix, one cytosolic α-helix, and an unstructured cytosolic carboxy terminus (Hicks *et al*., 2003). Its gene, *tatB*, is found in the same operon as the *tatA* and *tatC* genes. TatC consists of 6 transmembrane α-helices (Punginelli *et al*., 2007) and is found in the membrane with TatB in a 1:1 ratio (Bolhuis *et al*., 2001). TatA is smaller compared to TatB (Sargent *et al*., 1998), but has a similar secondary structure and shares 20 % sequence similarity with TatB (Hicks *et al*., 2003). TatC recognizes and binds the twin-arginine part of the signal peptide as shown by cross-linking experiments (Panahandeh *et al*., 2008). These

studies also showed that downstream parts of the signal peptide are bound by TatB. Tarry *et al.*, 2009 always isolated TatB and TatC together, which indicates that both these proteins are required for the initial recognition of the Tat signal peptide. TatA require a TatBC complex to oligomerize into a functional pore in the bacterial membrane (Leake *et al.*, 2008). The study by Leake *et al.*, 2008 revealed ring-shaped oligomers with an average of 25 TatA molecules in the IM. They speculate that after binding of the substrate by TatBC, TatA oligomerizes in the membrane around the substrate, creating a pore big enough to accommodate the substrate in question (Figure 3). During transport, TatC inserts the signal peptide in a binding pocket between TatB and TatC (Fröbel *et al.*, 2012). After the substrate has crossed the membrane, the signal peptide is made available to the signal peptidase LepB, which cleaves the signal peptide, and the substrate is released from the IM (Fröbel *et al.*, 2012).

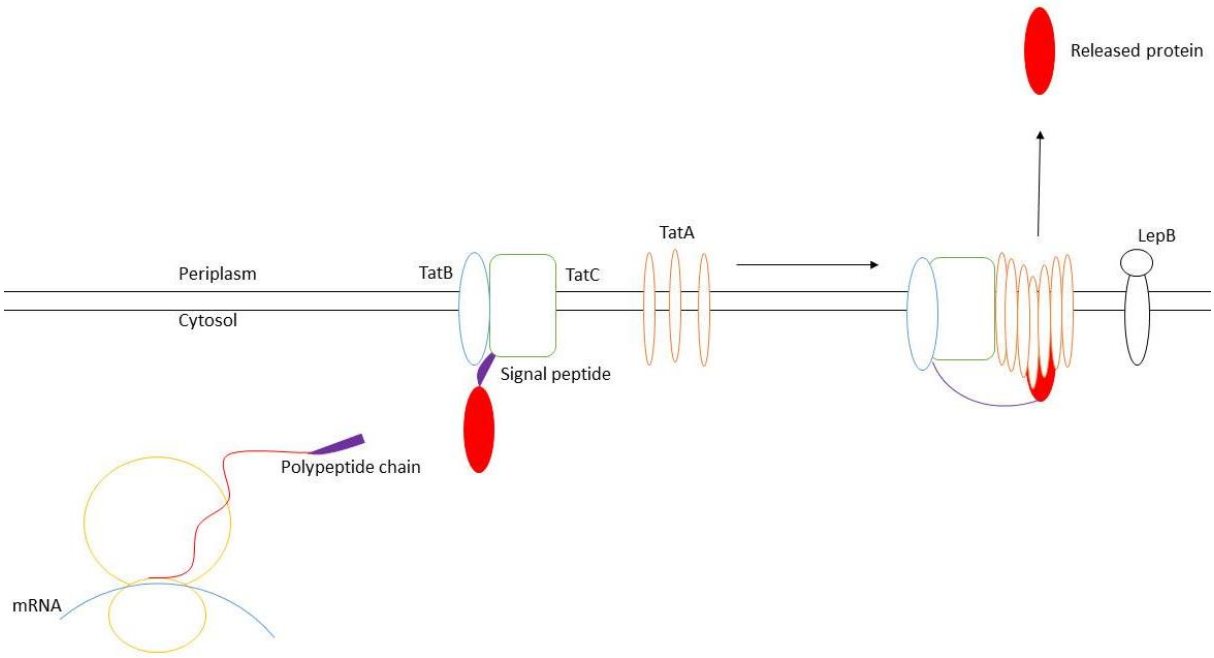

Figure 3: A simplified illustration of the Tat pathway (Panahandeh *et al.*, 2008, Tarry *et al.*, 2009, Leake *et al.*, 2008, Fröbel *et al.*, 2012); the protein is translated in the cytosol on a ribosome, and folds into its secondary and tertiary structure, including cofactor. The signal peptide is recognized and bound by the TatBC complex in the IM. This leads to oligomerization of TatA into a channel in the membrane, and the protein is translocated across. On the periplasmic side, the protein is released when the signal peptide is cleaved of by the signal peptidase LepB.

Transport to the outer membrane of *Escherichia coli*

The OM proteins of *E. coli* are β-barrels or lipoproteins, in contrast to the IM proteins which are either α-helical proteins or lipoproteins. New discoveries also revealed some OM proteins containing integral membrane domains made up of α-helices in the shape of a barrel (Dong *et al*., 2006). β-barrels are inserted into the OM by a protein complex called the β-barrel assembly machinery (BAM) after transport across the IM through the Sec translocase (Wu *et al*., 2005). As membrane proteins will have hydrophobic regions for membrane anchoring, they are prone to aggregation in the periplasm. The chaperones SurA (Sklar *et al*., 2007), Skp (Walton *et al*., 2009), and DegP (Subrini and Betton, 2009) bind proteins destined for the OM to avoid this aggregation. Sklar *et al.*, 2007 suggest that SurA is the most important chaperone when it comes to the assembly of β-barrels in the OM, and that Skp and DegP function as a helper pathway should a protein escape SurA. The chaperones deliver the OM protein to the assembly machinery, BAM, which consists of the central β-barrel protein BamA and associated lipoproteins BamB, BamC, BamD, and BamE, and the β-barrel is then properly folded and inserted into the OM.

The lipoproteins of the *E. coli* membranes are attached to the membrane through a lipid anchor consisting of three diacylglycerol chains covalently bound to the amino-terminal cysteine (C) (Sankaran and Wu, 1994). The C is found in the lipobox sequence leucine-[alanine/serine]-[glycine/alanine]-cysteine (L-[AS]-[GA]-C). Lipoproteins are produced in the cytosol with a signal sequence for transport across the IM, and a lipobox sequence. After translocation across the membrane, the anchoring to the three diacylglycerol chains and cleavage of the signal sequence is catalyzed in the outer leaflet of the IM by Lgt, LspA and Lnt. Lipoproteins lacking a Localization of lipoproteins (Lol)-avoidance signal, are then transferred to the OM (Masuda *et al*., 2002), while those containing an avoidance signal are retained in the IM. A Lol avoidance signal is recognized as an aspartatic acid (D) at the position next to the acetylated C residue (position 2) (Yamaguchi *et al*., 1988), and will also often require certain residues at position 3 such as glutamatic acid or glutamine (Hara *et al.*, 2003). Transfer to the OM is facilitated by the Lol system. The ABC transporter LolCDE binds the lipoprotein destined for the OM. When LolD hydrolyzes ATP, the lipoprotein is transferred to the periplasmic chaperone LolA (Yakushi *et al*., 2000), and then to the OM anchored lipoprotein LolB (Matsuyama *et al*., 1997). Finally, LolB transfers the lipoprotein to the OM (Yakushi *et al*., 2000).

1.2 Practical approach

The first aim of this project was to develop stable *E. coli* BL21 Gold (DE3) strains that express fluorescent biomarkers in both membranes. We also wanted to introduce these biomarkers into a knockout BL21 (DE3) strain, Δ *lamB, ompA, ompC, ompF* (ΔABCF) (Meuskens, 2015). The knock-out genes in this strain encode abundant OM proteins, and the idea behind the strain knock-out was to make room for overexpression of other OM proteins. With optimized expression levels of the membrane-bound fluorescent biomarkers, one can perform co-localization studies of bacterial membrane proteins. The biomarkers used in this project are mCherry (Shaner *et al*., 2004), superfolder Green Fluorescent Protein (sfGFP) (Pédelacq *et al*., 2006), and *Escherichia coli* Flavin mononucleotide binding Fluorescent Protein (EcFbFP) (Drepper *et al*., 2007). These fluorescent labels are directed to their respective membranes by fusion to proteins with known outer or inner membrane localization, or with an artificial signal sequence. For labelling the IM, the α-helical proteins Mistic (Roosild *et al.,* 2005) and pf3 (Kumazaki *et al.,* 2014) were used, while outer membrane protein A (OmpA) (Pautsch and Schulz 1998) and the artificial signal sequence Tat-lipobox (Blaudeck *et al.,* 2001) were used to direct the biomarkers to the OM.

1.2.1 Fluorescent biomarkers and their fusion partners

The fluorescent proteins

mCherry (Figure 4A) was developed by Shaner *et al.,* 2004 through several rounds of directed evolution from monomer Red Fluorescent Protein 1. These evolution rounds resulted in beneficial folding mutations, a shift in absorbed and emitted wavelengths, and increased tolerance of fusion proteins. According to Shaner *et al.*, 2004, mCherry has the best photostability, it is stable over a large pH range, and has the fastest maturation rate among commonly used fluorescent proteins. Experiments by Yu and Götz, 2012 show that mCherry can be successfully transported through the Sec translocase and be fully fluorescent in the periplasm. They also found that translocation of mCherry to the surface of the cell significantly reduced the fluorescence detected.

Pédelacq *et al*., 2006 generated sfGFP (Figure 4B) with a green fluorescent protein (GFP) containing the folding-promoting mutations F99S, M153T, and V163A, called the “cycle-3” mutations, and the enhanced GFP mutations F64L and S65T, as a starting point. The sfGFP

they created had six additional mutations: S30R, Y39N, N105T, Y145F, I171V, and A206V. Pédelacq *et al.*, 2006 showed that this GFP variant had a 50-fold higher fluorescence compared to the GFP variants with the cycle-3 mutations and the enhanced mutations. The group also tested renaturation after urea treatment, and sfGFP showed a significantly higher folding robustness compared to other GFP variants. The fluorescence after fusion to protein partners showed a direct correlation between the amount of expressed fusion proteins and the fluorescence measured. It has been shown that in contrary to GFP (Yu and Götz, 2012), sfGFP can be translocated successfully through the Sec translocase (Uehara *et al.*, 2010, Dinh and Bernhardt, 2011). An important aspect to keep in mind when working with GFP is that GFP can form biologically active inclusion bodies in the cell (Huang *et al.*, 2013). Inclusion bodies are aggregates of proteins, in this case in a loose heap mainly consisting of β-sheet structures.

The background for developing a flavin mononucleotide binding fluorescent protein (FbFP) was the fact that GFP, the common fluorescent label, require oxygen for fluorophore maturation. Drepper *et al.*, 2007 used the blue-light photoreceptors YtvA, from *Bacillus subtilis* (*B. subtilis*), and SB2, from *Pseudomonas putida*, to develop BsFbFP and PpFbFP, respectively. These proteins had enhanced fluorescence compared to the autofluorescence of the wild type proteins due to the mutation of the photoactive cysteine residues Cys62 (YtvA) and Cys53 (SB2) to alanine. Without these mutations, a covalent complex between cysteine and the excited flavin mononucleotide (FMN) would occur, and this photochemical cycle ultimately leads to photobleaching (Drepper *et al.*, 2007). EcFbFP (Figure 4C) used in this project, was developed by Drepper *et al.*, 2007, and consists of the 137 amino terminal residues of BsFbFP expressed with an *E. coli* codon bias. These residues encode the photoactive light oxygen voltage domain of *B. subtilis* YtvA with the Cys62Ala mutation. As FMN production does not require oxygen, EcFbFP is fluorescent under anaerobic conditions as well as aerobic conditions (Drepper *et al.*, 2007). Investigations by Mukherjee *et al.*, 2013 showed that EcFbFP is fluorescent over a broad pH range, and can restore fluorescence after denaturation (2 – 3 minutes) due to heat treatment at 90 °C for 25 minutes. These findings, the oxygen independent properties, and the small size of EcFbFP make it an excellent biomarker.

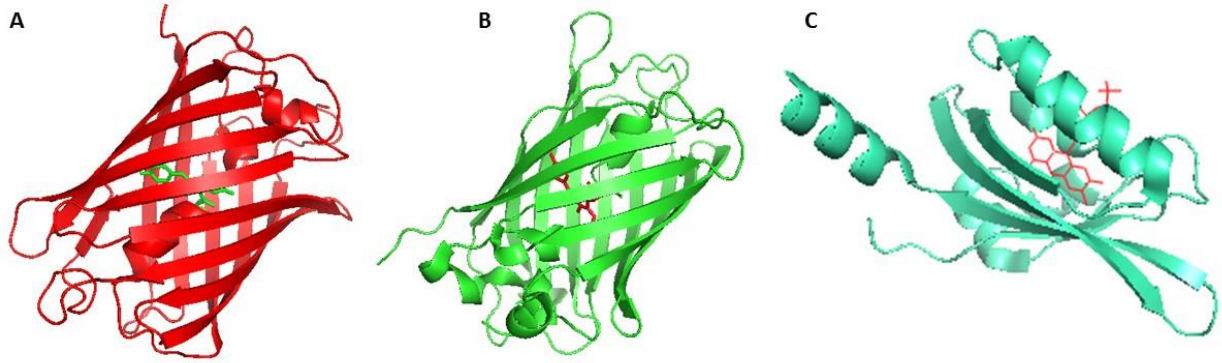

Figure 4: Crystal structures of the fluorescent proteins utilized in the project A) mCherry (PDB: 2H5Q) with chromophore in green. B) sfGFP (PDB: 2B3P) with chromophore in red. And C) EcFbFP (PDB: 2PR5 displays YtvA. To obtain the EcFbFP structure, the first 137 amino acid residues from YtvA were used) with FMN in red. The proteins are displayed with their fluorescent color, red, green and cyan, respectively.

The brightness of fluorescent proteins is dependent of several factors. These include maturation time, the protein expression level, the molar extinction coefficient value within the excitation wavelength range, and the quantum yield (Piston *et al.*). Accounting for the quantum yield and the molar extinction coefficient, the brightness of mCherry is 15 840 (Lambert and Thorn), the brightness of sfGFP is 54 145 (Lambert and Thorn), and the brightness of EcFbFP is 4250 (Mukherjee *et al.*, 2013). This shows that EcFbFP has a significantly lower brightness compared to the two other fluorescent proteins.

An additional factor to keep in mind when working with fluorescent proteins is autofluorescence – a weak fluorescence emitted naturally by cellular components such as flavoproteins which is excited at 488 nm (Benson *et al*., 1979), and β-Nicotineamide Adenine Dinucleotide (NADH) which is excited at 340 nm (Knight and Billinton, 2001).

The membrane bound fusion partners

The fusion partners for the fluorescent biomarkers were, as mentioned, Mistic, pf3, the artificial Tat-lipobox signal sequence, and OmpA. Mistic is a *B. subtilis* integral IM protein of 110 amino acids (Roosild *et al.*, 2005). In contrast to other integral membrane proteins, Mistic has a hydrophilic surface exposed in the membrane, while the internal part of the folded protein is hydrophobic (Roosild *et al.*, 2005). Mistic does not contain a signal sequence directing it to the IM, and is hence integrated into the membrane by a Sec-independent pathway. The mechanism of this integration is not known. Roosild *et al.*, 2005 used NMR to show that Mistic consists of a bundle of 4 α-helices in the IM (Figure 5A). The second helix,

labelled green in Fig. 5A, has a kink. In another study from 2006, Roosild *et al.*, 2006 found that the 84 carboxyl-terminal residues of Mistic, the core, are important for chaperoning recombinant IM proteins to the membrane. The full length protein requires detergents to be solubilized, while the shorter 84 residue version can be soluble in the cytoplasm *(Roosild et al.*, 2005).

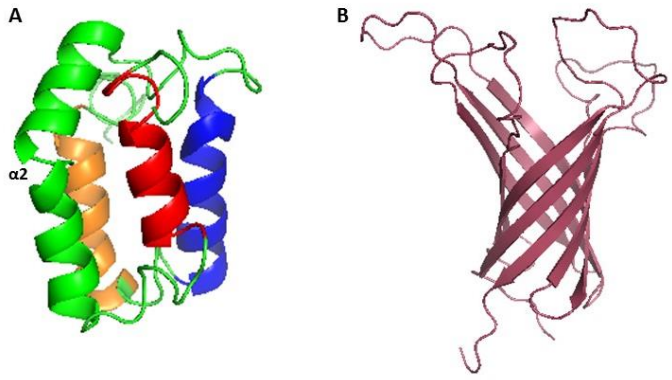

Figure 5: A) NMR structure of *B. subtilis* integral IM protein Mistic. The protein consists of a 4-helical bundle, where the second α-helix (labelled green) has a kink (PDB: 1YGM). B) NMR structure of the integral membrane domain of OmpA (PDB: 2GE4).

The *Pseudomonas aeruginosa* phage Pf3 coat protein is a small protein of 44 amino acid residues and consists of one transmembrane α-helix. The carboxyl-terminal, cytoplasmic region contains 8 amino acids, while the longer 18-residue amino-terminal region is located in the periplasm of *E. coli* (Kiefer *et al.*, 1997). This orientation in the membrane is due to charged residues flanking the membrane anchor (Kiefer *et al.*, 1997), where the correct orientation requires positively charged residues at the carboxyl-terminus and negatively charged residues at the amino-terminus. By reversing the charges in the flanking regions, Kiefer *et al.*, 1997 showed that the orientation of pf3 in the *E. coli* membrane was reversed. This study also found that the membrane potential is relevant for the insertion of pf3 in the membrane. It was the negatively charged residues on the amino terminus of the protein that responded to this potential. The actual insertion of pf3 into the IM is Sec-independent and controlled by the insertase YidC (Figure 6). Chen *et al.*, 2002 showed that in cells lacking YidC, pf3 was not inserted into the IM in the normal C_{in}/N_{out} orientation. The group also showed results indicating physical contact between the membrane anchor of pf3 and YidC during membrane insertion.

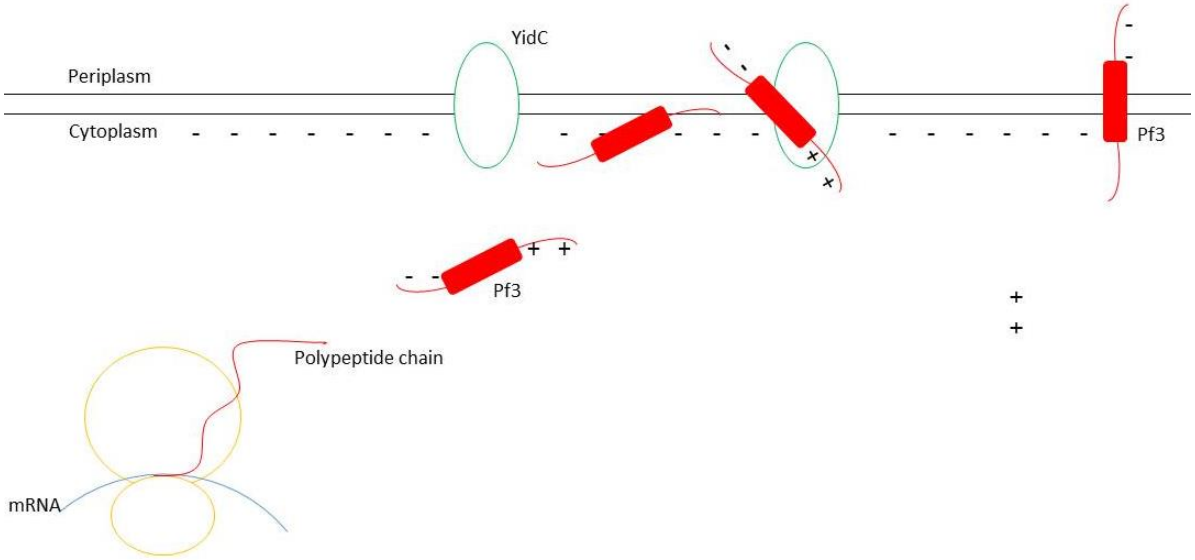

Figure 6: Pf3 is translated in the cytosol and interacts with the membrane before being picked up by YidC and inserted into the membrane in a C_{in}/N_{out} orientation with the aid from the membrane potential (Illustration based on Chen *et al.*, 2002).

The Tat-lipobox signal used to direct proteins to the OM in this project is an artificial signal sequence consisting of a Tat signal directing transport through the Tat translocase (Blaudeck *et al.*, 2001), and a lipobox signal for lipid anchoring in the OM through the Lol system (von Heijne, 1989). Blaudeck *et al.*, 2001 used the Tat signal sequence from the *E. coli* preTorA protein, an OM trimethylamine N-oxide reductase, to transport *Zymomonas mobilis* glucose-fructose oxidoreductase (GFOR) through the *E. coli* Tat translocase. This resulted in efficient protein transport across the IM compared to experiments when the native Tat signal sequence from GFOR was used. In this project, the sequence following the cleavage site indicated in Figure 7A in preTorA with a black arrow, was replaced with a lipobox indicated in bold letters in Fig. 7B (von Heijne, 1989) for transport and anchoring in the OM. A D was added following the C, making the sequence L-A-G-C-D. The new cleavage site is indicated with a black arrow in Fig. 7B. The twin arginine residues required for transport through the Tat translocase are indicated in red in both panels in Fig. 7.

A) PreTorA MNNNDLFQASRRRFLAQLGGLTVAGMLGPSLLTPRRATAAQA ATDAVISK...

B) Artificial Tat-lipobox MNNNDLFQASRRRFLAQLGGLTVAGMLGPSLLTPRRATAAQA**LAG CD**...

Figure 7: A) Signal peptide of preTorA with a twin arginine signal mediating transport through the Tat translocase in red, and the signal peptide cleavage site indicated by an arrow (Blaudeck *et al.*, 2001). B) The sequence following the cleavage site was replaced by the lipobox signal L-A-G-C-D. The new cleavage site is indicated with a black arrow.

OmpA is an integral OM protein of 325 amino acids, were the first 171 amino acids make up the membrane anchored domain (Pautsch and Schulz, 1998) (Figure 5B). This domain consists of an eight-stranded β-barrel with the carboxyl- and amino-termini located in the periplasm (Pautsch and Schulz, 2000). The periplasmic domain is globular and connects OmpA to the peptidoglycan layer in the periplasm (Rosenbusch, 1974). OmpA is important for the maintenance of the cellular shape of *E. coli* (Sonntag *et al*., 1978), and has been found to be released from the cell during host invasion (Hellman *et al.,* 2000). OmpA is fully translated in the cytosol and requires the chaperone SecB for delivery to the Sec translocase (Baars *et al.*, 2006). In this project, the integral membrane domain of OmpA as seen in Fig. 5B was used to direct a fluorescent label to the OM by replacing the globular periplasmic domain with a fluorescent protein.

Table 1 shows an overview of the fluorescent proteins and their fusion partners used in this project. A flexible linker peptide consisting of glycine-serine-glycine-serine (GSGS) was added between the fusion proteins to allow proper folding without interference from the fusion partner. The properties of the proteins discussed above made these combinations the most appropriate place to start.

Table 1: Fluorescent fusion proteins with target membrane and fluorescence excitation and emission wavelengths.

Fusion protein	**Target membrane**	**Excitation wavelength (nm)**	**Emission wavelength (nm)**
OmpA-mCherry	Outer membrane	587	612
Tat-lipobox-EcFbFP	Outer membrane	450	495
Mistic – EcFbFP	Inner membrane	450	495
Mistic – sfGFP	Inner membrane	485	510
Pf3 – EcFbFP	Inner membrane	450	495
Pf3 - sfGFP	Inner membrane	485	510

1.2.2 Gibson Cloning

The fusion of the DNA sequence encoding the fluorescent labels with the DNA sequence encoding the membrane proteins or artificial signal sequence were executed with the Gibson

Assembly® Cloning Kit from New England BioLabs® (NEB). The method was developed by Daniel G. Gibson *et al.*, 2009. This assembly technique evades the design of primers containing restriction sites, and reduces the work time by avoiding the restriction enzyme cutting step and the isolation of the modified DNA, proceeding directly to the ligation step. In addition, several DNA fragments can be cloned together simultaneously in one step. In place of including restriction sites, primers are designed to include overlaps between the sequences to be fused, and between the final fused sequence and the plasmid used for expression (Figure 8). The primers are then used to amplify the sequences separately, creating double stranded DNA (dsDNA) with overlapping ends. The amplified DNA and the linearized plasmid are finally mixed with the Gibson Assembly® Master Mix. The Gibson Assembly® Master Mix contains a 5' exonuclease (T5 exonuclease), Phusion DNA polymerase, and Taq DNA ligase (Gibson *et al.*, 2009). During incubation with the Master Mix, the exonuclease creates 3' single stranded overhangs on the ends of the dsDNA inserts and the linear plasmid. The overlapping sequences anneal, and the DNA polymerase will fill in gaps created by the exonuclease. Finally, the ligase seals the nicks, creating a circular plasmid with the desired fusion gene (Gibson *et al.*, 2009) (Figure 8). This method can also be used to create linear dsDNA. The only requirement is the overlapping sequences at the correct location.

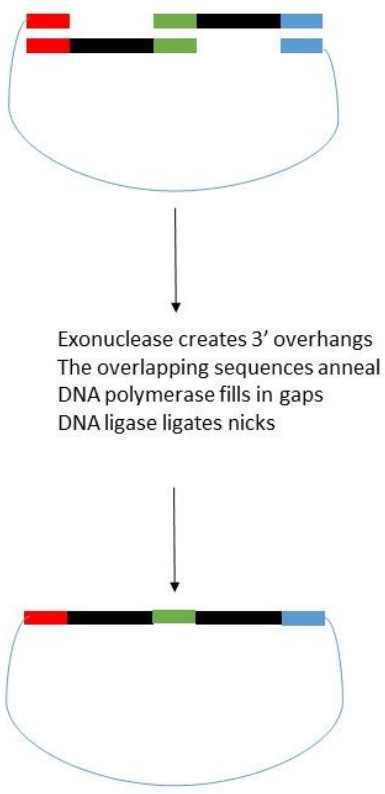

Figure 8: Illustration of the Gibson Assembly® Cloning Kit from NEB. Amplified dsDNA, constructed with overlapping sequences and the linearized plasmid are incubated with the Gibson Assembly® Master Mix. In the tube, the exonuclease creates 3' single stranded overhangs, the overhangs anneal, the DNA polymerase fills in the gaps, and the DNA ligase ligates the nicks. The product is a circular plasmid containing the fusion gene (Gibson *et al.*, 2009).

1.2.3 λ Red Recombination

λ red recombination is used as a simple, quick tool for genetic engineering (Datsenko and Wanner, 2000). Shortly, linear, dsDNA is transformed into induced cells carrying a helper plasmid with the λ red genes. The three proteins encoded by the plasmid are expressed and facilitate the integration of the dsDNA into the chromosome of the cell using homologous recombination. All that is required for this event is 36 – 70 nucleotides of homology between the genome and the flanking regions of the dsDNA (Datsenko and Wanner, 2000). For this project, we chose the AttB site (Misra *et al*., 2015) and one of the three asparagine tRNA genes, *AsnU*, (Buchrieser *et al*., 1998) in the *E. coli* BL21 Gold (DE3) genome as the insertion sites for the fusion proteins (for the homologue genome sequences, see Appendix 3).

The λ red recombination system utilizes three of the *E. coli* phage λ proteins from the P_L operon, Exo, Bet and Gam. These are part of the early expressed proteins in the phage λ infection cycle. The *exo* gene translates to a λ exonuclease that creates 3' single stranded overhangs in the dsDNA transformed into the cell (Little, 1967). β protein, encoded by *bet*, is a single stranded DNA (ssDNA) binding protein that binds the 3' overhangs created by the λ exonuclease (Kmiec and Holloman, 1981). Kmiec and Holloman 1981 found that the β protein binds the ssDNA and catalyzes annealing with homologous sequences. This annealing takes place during replication, when the strands are separated by the replication fork. Finally, the product of the *gam* gene, γ, is found in the cell as a dimer and binds RecBCD and stalls its activities (Murphy, 1991). RecBCD is a helicase with a main function to use homologous recombination to repair double stranded breaks in *E. coli* (Dillingham and Kowalczykowski, 2008).

The dsDNA that was introduced into the *E. coli* genome with λ red recombination in this project contained a promoter, a fusion gene, a terminator, and a kanamycin cassette with flanking Flp recombination target (FRT) sites (Baba *et al.*, 2006). Three promoters were chosen to optimize the expression of fluorescent proteins in the strains – an L-arabinose inducible promoter (Invitrogen, 2010), a strong constitutive promoter, and a weak constitutive promoter. Both constitutive promoters were from the Anderson collection (Anderson).

Removal of the kanamycin cassette from the *E. coli* genome after λ red recombination

As the fluorescent strains made in this project are to be used for membrane protein expression in the future, it is not favorable to keep the kanamycin cassette in their genomes. As plasmids used for protein expression often has an antibiotic resistance gene for easy selection, an additional resistance gene in the genome is not advantageous. The kanamycin cassette used for the simple selection of recombinant clones after λ red recombination are from the Keio collection by Baba *et al.*, 2006. The cassette is flanked by FRT sites. FRT sites are 65 bp sequences recognized by the yeast *Saccharomyces cerevisiae* Flp recombinase (Cox, 1983). The Flp recombinase binds these recognition sites and catalyzes the recombination between them, resulting in the excision of the DNA in between (Cox, 1983). The result is a "scar" in the DNA containing one FRT site. By transforming the recombinant cells with the pCP20 plasmid which contains the gene for the Flp recombinase (Cherepanov and Wackernagel, 1995), and inducing expression from the plasmid, the resistance cassette is removed from the genome.

1.2.4 Membrane isolation

To verify the localization of the fluorescent membrane labels, two different membrane separation techniques were utilized. The selective detergent treatment technique uses lauroyl sarcosine to selectively solubilize the inner membrane, while the density gradient centrifugation technique separates the membranes based on the different densities of the inner and the outer membranes. The first step of both techniques is to lyse the bacterial cells, creating small membrane vesicles. For selective detergent treatment, glass beads are added to the bacteria, which are then beaten in a homogenizer, resulting in cell lysis and creation of the membrane vesicles. For the density gradient separation technique, a French pressure cell was used. This forces the bacterial cells through a small opening with high pressure, which results in cell lysis. Membranes are best pelleted using an ultracentrifuge, centrifuging at a minimum of 100 000 x *g*. Once the membranes are collected, lauroyl sarcosine is used to solubilize the inner membrane in the selective detergent treatment method (Filip *et al.*, 1973). The mechanism behind this selective solubilization is unknown. In the density gradient centrifugation, the pelleted membranes are loaded on a sucrose gradient and centrifuged with a high force. This drives the membrane vesicles through the gradient, only stopping at the equilibrium – where the density of the gradient matches the density of the vesicles. As the

OM has a higher density compared to the IM, the membrane fractions are found in two separate bands in the gradient. This difference in density is due to the high content of LPS in the OM *(*Smit *et al*., 1975).

2 Materials and methods

2.1 Genetics

2.1.1 Primers

All primers, unless otherwise indicated, were designed manually and produced by LifeTechnologies™. The primer sequences can be found in Appendix 2.

2.1.2 Plasmids

A summary of the plasmids used in this project can be found in Table 2 below. pACYCDuet-1 was utilized for cloning. It contains a T7 RNA polymerase promoter for efficient and high expression of the desired proteins, 2 multiple cloning sites, and a chloramphenicol resistance gene for selection. pKD46, pSIM8, and pSIM9 all contain the λ red genes used for λ red recombination. pKD46 has an ampicillin resistance gene, and an L-arabinose inducible promoter controlling the expression of the λ red genes. Both pSIM plasmids have an antibiotic resistance gene, and the expression of the λ red genes is induced by a temperature increase from 30 °C to 42 °C. This rise in temperature deactivates the heat-sensitive repressor cI857. The repressor is active at low temperatures of 30 – 34 °C and inhibits transcription of the λ red genes from the promoter. When the temperature is increased to 42 °C, the repressor is inactivated and the λ red genes are transcribed with high efficiency. When the temperature is lowered again, the repressor is reactivated and the expression is turned off (Sharan *et al.*, 2009, Datta *et al.*, 2006). Usage of pCP20 can be found in section 2.6.

Table 2: Overview of the plasmids utilized in this project. The table includes purpose, growth temperature, antibiotic resistance gene, and origin. *information on pCP20 can be found in sections 1.2.3 and 2.6.

Name	**Purpose**	**Growth temperature**	**Resistance**	**Origin**
pACYCDuet-1	Cloning	37 °C	Chloramphenicol	Novagen
pKD46	λ red recombination	30 °C	Ampicillin	Datsenko and Wanner, 2000
pSIM9	λ red recombination	30 °C	Chloramphenicol	Datta, *et al.*, 2009

pSIM8	λ red recombination	30 °C	Ampicillin	Datta, *et al.*, 2009
pCP20	Excision of Km cassette through FRT sites*	30 °C	Ampicillin	Datsenko and Wanner, 2000

2.1.3 Polymerase Chain Reaction

Polymerase Chain Reaction (PCR) is a method used for DNA amplification. It consists of cycles of different temperatures where the template DNA to be amplified is denatured to create ssDNA, complementary primers anneal with the template, and a DNA polymerase creates a new strand by primer extension. PCR reactions were performed according to the manufacturer's protocols. All polymerases, dNTPs and corresponding buffers used in the PCR protocols described below were from NEB.

Cloning of fusion proteins

For amplification and cloning purposes, Phusion®High-Fidelity DNA Polymerase was used due to its low error rate and high processivity. A 50 µl reaction contained 10 µl 5X Phusion HF buffer, 1 µl 10 mM dNTPs, forward and reverse primers to a concentration of 0.5 µM, 10 ng template, 0.5 µl Phusion®High-Fidelity DNA Polymerase, and distilled H_2O to 50 µl. The reactions were performed using a Biometra Personal Thermocycler (from Analytik Jena) with the following program:

Denaturation	98 °C	30 sec
Denaturation	98 °C	10 sec
Annealing	60 °C	30 sec
Elongation	72 °C	30 sec per kilobase / Return to step 2 24 times
Final elongation	72 °C	5 min
Pause	12 °C	∞

To eliminate plasmid carryover when a plasmid was utilized as the template for the PCR reaction, the PCR products were treated with DpnI from NEB. DpnI is a restriction enzyme that recognizes and cleaves methylated GATC sequences, and will hence remove the plasmid

template from the PCR reaction. The PCR product will not be affected, as this DNA is not methylated. For a digestion reaction, 0.5 µl DpnI was added to the PCR mix and incubated at 37 °C for 1 hour. Finally, the digested reaction was purified (section 2.1.6).

Colony PCR

As the error rate of the polymerase was unimportant for colony PCR, Taq DNA polymerase was used for this purpose. A master mix containing 2.5 µl 10x Standard Taq Reaction Buffer, 0.5 µl 10 mM dNTPs, forward and reverse primers to 0.2 µM, 0.2 µl Taq DNA polymerase, and distilled H_2O to 25 µl per colony to be investigated, were made. The master mix was aliquoted to 25 µl in PCR tubes, and colonies were transferred from a plate to the tubes. The reactions were performed using a Biometra Personal Thermocycler (from Analytik Jena) with the following program:

Cell lysis	95 °C	3 min
Denaturation	95 °C	30 sec
Annealing	50 °C	30 sec
Elongation	68 °C	1 minute per kilobase / Return to step 2 24 times
Final elongation	68 °C	5 min
Pause	12 °C	∞

Splicing by Overlap Extension

In order to join two PCR products together, Gibson Assembly (section 2.1.4) or Splicing by Overlap Extension (SOEing) were used (Figure 9). SOEing requires that the two PCR products to be joined together have overlapping sequences of 15-20 nucleotides. This was achieved through primer design. A reaction of 50 µl contained 10 ng of each PCR product, 10 µl 5X Phusion HF buffer, 1 µl 10 mM dNTPs, 0.5 µl Phusion®High-Fidelity DNA Polymerase, and distilled H_2O to 50 µl. In the first 10 cycles of the SOEing, an annealing temperature of 45-50 °C was used. In this part, primers were absent from the mix, and the overlapping sequences of the two PCR products to be joined annealed and acted as the primers for the DNA polymerase (Figure 9). The low temperature ensured annealing between

the complementary sequences, and therefore product formation. After 10 cycles, the forward primer for the 5' construct and the reverse primer for the 3' construct were added to a concentration of 0.5 µM, and a standard PCR program was applied. The reactions were performed using a Biometra Personal Thermocycler (from Analytik Jena) with the following program:

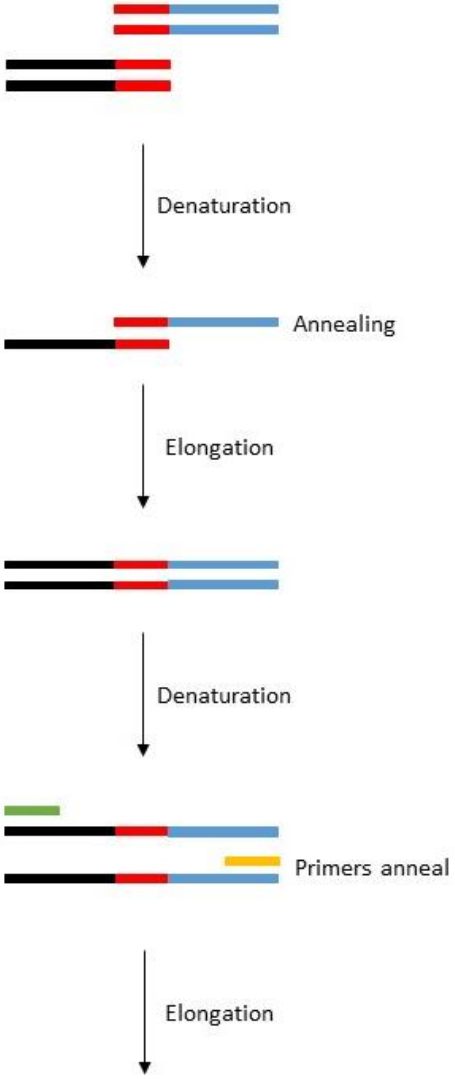

Denaturation	98 °C	30 sec
Denaturation	98 °C	10 sec
Annealing	45 °C	30 sec
Elongation	72 °C	30 sec per kilobase /
		Return to step 2 10 times
Denaturation	98 °C	10 sec
Annealing	60 °C	30 sec
Elongation	72 °C	30 sec per kilobase /
		Return to step 5 24 times
Final elongation	72 °C	5 min
Pause	12 °C	∞

Figure 9: Illustration of SOEing.

2.1.4 Cloning with Gibson Assembly

The Gibson Assembly® Master Mix from NEB was used in the cloning process in order to join two PCR products with overlapping ends. The primers used to amplify the PCR products were designed to contain overlapping ends with each other and, in instances where the products were to be cloned into a plasmid, the plasmid. For an illustration of this, see the

introduction, Fig. 8, section 1.2.2. The reaction was assembled on ice in an 1.5 ml Eppendorf tube. In the reaction, 100 ng of the linearized vector was mixed with 200 ng of inserts of > 200 base pairs, and 500 ng inserts of < 200 base pairs. An equal volume of the Master Mix was added, and the reaction was incubated at 50 °C for 15 minutes. After incubation, 2 µl of the reaction mix was used to transform *E. coli* TOP10 cells (section 2.2.4). Table 3 shows an overview of the fusion genes joined together and cloned into pACYCDuet-1 with Gibson Assembly. All fusion genes were cloned into the first multiple cloning site of pACYCDuet-1 using the primers pACYCDuetMCS1 Fwd and pACYCDuetMCS1 Rev. Primers used for cloning OmpA-mCherry into the second multiple cloning site were pACYCDuetMCS2 Fwd, pACYCDuetMCS2 Rev, OmpA MCS2 Fwd, and mCherry MCS2 Rev (Appendix 2).

Table 3: An overview of constructs and primers used for amplification of the genes. All constructs in the table were cloned into the first multiple cloning site of pACYCDuet-1

Construct	**Primers for amplification of genes**
OmpA-mCherry	OmpA Fwd, GSGS ompA rev, OmpA-mCherry Fwd, mCherry Rev
Tat-lipobox-EcFbFP	Tat-lipo Fwd, Tat-lipo Rev, Tat-EcFbFP Fwd, EcFbFP Rev
Mistic-EcFbFP	Mistic Fwd, Mistic Rev, Mistic-EcFbFP Fwd, EcFbFP Rev
Mistic-sfGFP	Mistic Fwd, Mistic Rev, Mistic-sfGFP Fwd, sfGFP Rev
Pf3-EcFbFP	Pf3 Fwd1, Pf3 Rev1, Pf3 Fwd2, EcFbFP-pf3 Rev2, EcFbFP Fwd, EcFbFP Rev
Pf3-sfGFP	Pf3 Fwd1, Pf3 Rev1, Pf3 Fwd2, GSGS pf3 Rev2, pf3-sfGFPF Fwd, sfGFP Rev

2.1.5 Agarose gels for DNA separation

1 % agarose gels were used to verify the sizes of the PCR products. These were made with agarose, 1xTBE buffer, and SYBR® safe for DNA staining (Appendix 4, Table 1), and the gels were run with 1xTBE buffer. The DNA was loaded onto the gels with DNA loading buffer (Appendix 4, Table 1). The DNA ladders used were a 1 kilo base ladder and a 100 base

pair ladder, both from NEB. The gels were run with a VWR 250 V Power Source with a constant voltage of 80 V for approx. 25 minutes.

2.1.6 Kits for DNA and plasmid isolation and PCR cleanup

The kits used for plasmid isolation, and gel and PCR clean-up were NucleoSpin Plasmid, and NucleoSpin Gel and PCR Clean-up, respectively. These are manufactured by Macherey-Nagel GmbH & Co.

2.1.7 Sequencing

In order to verify the cloning of fusion genes into pACYCDuet-1 after Gibson Assembly or into the *E. coli* genome after λ red recombination, samples were sent for sequencing to GATC Biotech. One tube contained 100 ng (purified plasmid) or 80 ng (purified PCR product) of the DNA to be sequenced, and a sequencing primer (Appendix 2) at a concentration of 5 µM. The total volume was 10 µl. The laboratory uses the LightRun^{TM} sequencing service at GATC Biotech, which is Sanger Sequencing based (Sanger and Coulson, 1975). The program ApE was used to analyze the sequencing results (Davis, 2013).

2.2 Bacterial methods

2.2.1 Bacterial strains

E. coli strains used in this project were TOP10 (LifeTechnologies^{TM}) for cloning purposes, and BL21 Gold (DE3) (AgilentTechnologies) and BL21 (DE3) ΔABCF (Meuskens, 2015) for expression studies. The TOP10 strain is optimized for cloning purposes, BL21 Gold (DE3) is optimized for protein expression, and BL21 (DE3) ΔABCF is optimized for overexpression of OM proteins.

2.2.2 Growth media and agar plates

Lysogeny broth (LB) (Bertani, 1951) was used as a growth media for all *E. coli* strains in this project. The BL21 (DE3) knockout ΔABCF require a low salt LB for growth. For components in LB, see Appendix 4, Table 2. For growth on plates, LB agar (Appendix 4, Table 3) with the appropriate antibiotic (section 2.2.3) was used.

2.2.3 Antibiotics

Antibiotics were used as a method of selection in overnight cultures and in LB agar plates. See Table 4 for stock- and working concentrations.

Table 4: Antibiotics used in project with stock- and working concentrations.

Antibiotic	**Stock concentration (mg/ml)**	**Working concentration (µg/ml)**	**Company**
Ampicillin	100	100	AppliChem
Chloramphenicol	25	25 (12,5 for pSIM9)	AppliChem
Kanamycin	50	50	AppliChem

2.2.4 Competent cells and transformation

Chemically competent cells and chemical transformation

Chemically competent cells were made by growing bacterial cells to an optical density (OD_{600}) of 0.3-0.5. Cells were collected by centrifugation (Eppendorf Centrifuge 5415 D) for 10 minutes at 4000 x *g*, resuspended in ¼ of the original volume of ice-cold 0.1 M $CaCl_2$ (Merck), and incubated on ice for 30 minutes. Cells were pelleted at 4 °C at 4000 x *g* and resuspended in 1/25 of the original volume in ice-cold 0.1 M $CaCl_2$. Finally, an equal volume of ice-cold 60 % glycerol (VWR AnalaR Normapur) was added to the cells. The cells could be used directly for transformation or stored at -80 °C.

2 µl of the Gibson Assembly Mix after Gibson Assembly, or 50 ng of plasmid were used to transform *E. coli* TOP10, BL21 Gold (DE3), and BL21 (DE3) ΔABCF. Chemically competent cells were aliquoted into 50 µl, and plasmid was added. After 30 minutes incubation on ice, heat shock was performed for 45 seconds at 42 °C. 2 minutes on ice was followed by the addition of 1 ml LB with 10 mM $MgSO_4$ (Merck). At the end of 60 minutes recovery incubation at 30 °C or 37 °C depending on plasmid specification, the cells were pelleted by a 2 minute centrifugation at 5600 x *g*. The pelleted cells were resuspended in 100 µl media, plated on LB plates with the appropriate antibiotic, if necessary, and incubated at 37 °C or 30 °C over night. See Table 2, section 2.1.2 for plasmid specifications for temperature.

Electro-competent cells and electroporation

Electro-competent cells were made by collecting cells at OD_{600}=0.3-0.5. Aliquots of 1 ml were transferred to 1.5 ml Eppendorf tubes, and the cells were pelleted and washed twice with ice-cold distilled H_2O. The final cell pellet was resuspended in 50 µl ice-cold distilled H_2O. All centrifugations were done at 4 °C and with 4000 x *g* (Eppendorf Centrifuge 5415 D). The electro-competent cells could be used immediately or stored at -80 °C. For storage, 60 % glycerol was added in the last step in place of distilled H_2O.

For transformation by electroporation, 0.5 µg DNA was added to an aliquot of 50 µl cells. The mix was transferred to a Gene Pulser® cuvette (0.2 cm electrode gap, BioRad) and electroporated at 2500 V in Eppendorf electroporator 2510 (capacity of 10 µF, resistance of 600 ohms). 1 ml room temperature LB with 10 mM $MgSO_4$ (Merck) was added, and the cells recovered for 60 minutes with 500 rpm shaking at 30/37 °C (Thermo-Shaker, HC24, Grant-bio) before being plated on LB plates with the appropriate antibiotics.

2.2.5 Induction of protein expression

All induction cultures in this project were grown at 26 °C.

Isopropyl β-D-1-thiogalactopyranoside induction

Isopropyl β-D-1-thiogalactopyranoside (IPTG) (G Biosciences®) induction was used to induce the expression of the T7 RNA polymerase from the *lac* promoter in the BL21 Gold (DE3) genome. Cells were grown to an OD_{600} of 0.3 and IPTG to a concentration of 0.25 or 0.50 mM was added to the culture. When the cell culture reached an OD_{600} of 2.0-2.5, the cells were collected for membrane separation (sections 2.3).

Autoinduction media

ZYP-5052 (Studier, 2005) was the autoinduction media (Appendix 4, Table 4) used for expression from the *lac* promoter in BL21 Gold (DE3). Activation of transcription from the promoter produced the T7 RNA polymerase that was required for transcription from the T7 promoter in pACYCDuet-1. The 5052 solution contained glucose, glycerol and lactose, which functioned as the carbon source for the bacteria. Glucose was first utilized, hence repressing the breakdown of lactose, and the induction from the *lac* promoter. This allowed the cells to

grow to a higher density before protein expression was induced. When the glucose level dropped, glycerol and lactose were utilized as carbon sources, and expression from the *lac* promoter was induced. Autoinduction was used due to its simplicity and the higher protein yield compared to IPTG induction.

2.3 Membrane separation methods

Two separation techniques were utilized in this project. The first technique was based on the solubilization of the IM with a selective detergent, while the second was based on the density difference between the two membranes, making it possible to separate them with density gradient centrifugation. Both membrane separation techniques used in this project was based on "Efficient subfractionation of Gram-negative bacteria for proteomics studies" by Thein *et al.*, 2010. All buffers and solutions used in the two membrane separation techniques described can be found in Appendix 4, Table 5.

2.3.1 Membrane separation based on selective detergent treatment

E. coli BL21 Gold (DE3) was grown over night in autoinduction medium (section 2.2.5). Cells corresponding to an OD_{600} of 0.6 were collected and diluted to 20 ml (for calculations, see section 2.7.1). The cells were pelleted and washed with ice-cold 10 mM HEPES pH 7.4 with 10 mM $MgSO_4$. The resuspended cells were transferred to tubes containing glass beads (Carl Roth GmbH+Co, KG) and lysed using a cell disruptor (SpeedMill PLUS from Analytik Jena). Cells were lysed with two rounds of shaking for 3 minutes with 3-minutes pauses between. A pinch of DNase I and Lysozyme to 0.1 mg/ml were added to the cell lysis tubes as tools to degrade DNA and break down the cell walls, respectively. These were both purchased from AppliChem. The tubes were centrifuged for 2 minutes at 4000 x *g* to remove cell debris, and the supernatant was transferred to a 2 ml Eppendorf tube. Thereafter, the tubes were centrifuged for 30 minutes at 15 600 x *g* to pellet the membranes. The membranes were then resuspended in 0.2 ml 10 mM HEPES pH 7.4. After the addition of 0.2 ml 2 % lauroyl sarcosine in 10 mM HEPES pH 7.4, the tubes were incubated with 500 rpm shaking at room temperature for 30 minutes. Another 30-minutes centrifugation at 15 600 x *g* pelleted the OM, which was washed in 0.5 ml 10 mM HEPES pH 7.4 and then resuspended in 60 µl 10 mM HEPES pH 7.4. The supernatant, containing the IM fraction, was also collected.

Samples were collected from the total lysate, and the inner and the outer membrane fractions for both fluorescence measurements and SDS-PAGE. Fluorescence measurements were done with a plate reader (Biotek Synergy MX platereader) in 96 well black plates (microplate, fluotrac 200, Greiner Bio One) using the program Gen5 1.10. For excitation and emission wavelengths corresponding to the fluorescent proteins, see Table 1, section 1.2.1.

I also attempted to use this separation technique with an ultracentrifuge for membrane pelleting. For this purpose a Beckman Coulter Optima^{TM} MAX Ultracentrifuge with the rotor MLA-80 and 10 ml Polycarbonate tubes (Beckman Coulter) were utilized at 100 000 x *g*.

2.3.2 Membrane separation based on density gradient centrifugation

Cells from ½ l autoinduced overnight culture or cells induced with IPTG (section 2.2.5) were ruptured in a French pressure cell with two passes at 10^8 Pa (Thermo IEC. FRENCH pressure cell press), and unbroken cells were removed by centrifugation at 4000 x *g* for 10 minutes. The crude membranes were pelleted at 250 000 x *g* in Beckman Coulter Optima^{TM} MAX Ultracentrifuge with the rotor MLA-80 and 10 ml Polycarbonate tubes (Beckman Coulter) for 1 hour, and resuspended in 2 ml 10 mM Tris pH 7.5, 15 % sucrose, 5 mM EDTA, and 0.2 mM DTT. The sucrose gradient consisted of layers of 2.4 ml of 50%, 45%, 35% and 30% sucrose in 10 mM Tris-HCl pH 7.5 and 5 mM EDTA. These were layered on a cushion of 1 ml 55% sucrose in 10 mM Tris-HCl pH 7.5 and 5 mM EDTA. After layering 1 ml of the membrane suspension on top of the gradient, the tubes were centrifuged for 16 hours at 250 000 x *g* in a Beckman Coulter Optima^{TM} LE-80K Ultracentrifuge with the hanging bucket rotor SW 41 Ti and 13.2 ml Ultra-Clear^{TM} centrifuge tubes (Beckman Coulter). Visible bands were collected with BD Plastipak 5 ml syringes with MEDICOR tips, and diluted to 6 ml with distilled H_2O for three rounds of washing. For this purpose, a Beckman Coulter Optima^{TM} MAX Ultracentrifuge with the rotor MLA-80 and 10 ml Polycarbonate tubes (Beckamn Coulter) were utilized at 100 000 x *g*. Sometimes, a third middle band was observed in the gradient. This was a mixed band and could be discarded (Thein *et al*., 2010). All centrifugation steps were performed at 4 °C.

Samples were collected of the total lysate, and the inner and the outer membrane fractions for both fluorescence measurements and SDS-PAGE. Fluorescence measurements were done as described above in section 2.3.1.

Optimization of the density gradient centrifugation method

At the end of the project, it was attempted to optimize the density gradient centrifugation method. By treating the lysate with lysozyme to break down the peptidoglycan of the *E. coli* periplasm, we ensured that the membrane vesicles did not stick together. This protocol was based on the cell lysis protocol using lysozyme from Sigma-Aldrich (Sigma-Aldrich). The lysate was incubated at 26 °C with 0.1 mg/ml lysozyme (AppliChem) for 15 minutes. The membranes were then separated as described above, but with two additional steps: a centrifugation step at 10 000 x *g* for 20 minutes after lysozyme treatment to remove inclusion bodies, and three washes of the pelleted membranes with a solution of 10 mM HEPES pH 7.4 and 1 M NaCl (VWR chemicals). The high salt content of this buffer was used to reduce unspecific interactions.

2.4 Polyacrylamide gels for protein separation

Polyacrylamide gels were used to separate proteins in the membrane fractions according to size. Table 6 in Appendix 4 lists chemicals required to make a stack of four 15 % polyacrylamide gels. The stacking gel was used to align the proteins in the sample, while the separation gel was used to separate the proteins according to size. The protein ladder used was PageRuler Prestained Protein Ladder, 10 – 180 kilo Daltons (kDa) from Life Technologies™. Gels were loaded with 10-15 µl protein sample and run at a constant current of 30 mA with a VWR 300 V Power Source. The protein samples were boiled for 10 minutes in 1 X SDS-PAGE sample buffer before being loaded onto the gel, and the polyacrylamide gels were run in 1 X SDS-PAGE running buffer (Appendix 4, Table 7).

2.4.1 Coomassie staining of SDS-PAGE gels

Coomassie Brilliant Blue R250 stain was used to stain SDS-PAGE gels to visualize proteins. Gels were stained over-night, then kept in destain solution until protein bands were visualized. The content of the stain and the destain solutions can be found in Appendix 4, Table 8.

2.4.2 Silver staining of SDS-PAGE gels

Silver staining is a sensitive method that requires a small amount of sample. In addition to staining proteins in the gel, the LPS in the samples are visualized. As these are found in the OM of *E. coli*, this staining method was used to investigate the presence of LPS in the membrane fractions after membrane separation. After separating the membrane fractions in a polyacrylamide gel (0.8-1 µl of each sample), the protocol in Table 5 was used as described by Nesterenko *et al.*, 1994. All steps were performed at room temperature. The solutions for the silver staining can be found in Appendix 4, Table 9.

Table 5: Protocol for silver staining of SDS-PAGE gels to visualize the LPS in the membrane fractions (Nesterenko *et al.*, 1994).

Step	**Time**
Fixation	5 minutes
Rinse	3 x 5 seconds
Wash	5 minutes
Rinse	3 x 5 seconds
Pretreat	5 minutes
Pretreat	1 minute
Rinse	3 x 5 seconds
Impregnate	8 minutes
Rinse	2 x 5 seconds
Develop	10 – 20 seconds
Stop	30 seconds
Rinse	10 seconds

2.4.3 Western blot

In a Western blot, proteins separated in a SDS-PAGE gel are transferred to a membrane, and the membrane treated with antibodies to visualize a protein of interest. Western blot using an

antibody against the OM protein OmpX was used as another method to verify the membrane separations. After a membrane separation, the membrane fractions were run in a polyacrylamide gel as described in section 2.4. The gel was then equilibrated in Western transfer buffer (Appendix 4, Table 10) for 5 minutes. A PVDF Transfer Membrane (Thermo Scientific) was cut to the same size as the gel, activated in isopropanol (Sigma-Aldrich) for 5 minutes until slightly translucent, and equilibrated in Western transfer buffer for 5 minutes. Six filter paper sheets (VWR) were cut to the same size as the gel, and soaked in the transfer buffer with the PVDF membrane. The transfer stack consisted of 3 layers of filter paper, the PVDF membrane, the gel, and another 3 layers of filter paper. Proteins were transferred to the PVDF membrane in TE70X semi-dry transfer unit from Hoefer using 65 mA and maximum voltage of 30 V for 50 minutes. After the transfer, the membrane was blocked in PBST with 2 % Bovine Serum Albumin (BSA) overnight (Appendix 4, Table 10). Anti-OmpX from rabbit (Arnold *et al*., 2007) was diluted 1:5000 in PBST with 2 % BSA and the membrane was incubated in this antibody solution for 1 hour. Hereafter followed a washing step with PBST for 10 minutes, and a 1 hour incubation with the secondary antibody (Goat anti-rabbit, Santa Cruz Biotechnology) in PBST with 2 % BSA. Another washing step with PBST followed, and finally detection with horseradish peroxidase using the protocol provided by the manufacturer (Pierce^{TM} ECL Western Blotting Substrate from Thermo Scientific). Kodak Image Station 4000R and the computer program Carestream MI SE were utilized to image the developed membrane.

2.5 β-Nicotineamide Adenine Dinucleotide oxidase enzymatic assay

To verify membrane separations, an enzymatic assay for the IM enzyme NADH oxidase was used. The most interesting fraction after membrane separation for our purposes was the OM fraction, as this contains the surface proteins and lipids of the bacteria, which are used in processes such as infection and adhesion. Hence, we wanted to test the fractions for the activity of an IM enzyme to investigate the purity after membrane separation. The protocol used was as described by Sigma Aldrich (Reusch and Burger, 1974), the solutions and their concentrations used are listed in Appendix 4, Table 11. In the reaction mix, any NADH oxidase present will oxidase NADH to NAD^+, resulting in a reduced absorbance at 340 nm.

1.9 ml deionized water, 0.6 ml potassium phosphate buffer, 0.3 ml Flavin Adenine Dinucleotide, and 0.1 ml NADH was added to a quarts cuvette (Hellma Analytics, Quartz Suprasil, 10 mm), and equilibrated to 30 °C. The absorbance at 340 nm was monitored (Agilent Technologies, G1103 with the computer program UV-vis 1/on) until constant, and a membrane fraction diluted in 30 mM potassium phosphate buffer with 0.1 % BSA, pH 7.5 was added to the reaction mix. The absorbance at 340 nm was recorded for 5 minutes. As a control, 30 mM potassium phosphate buffer pH 7.5 with 0.1 % BSA without membrane fraction was used.

2.6 λ Red Recombination

λ red recombination was used to transfer the constructs containing the fusion genes with a promoter, a terminator and a kanamycin cassette into the *E. coli* BL21 Gold (DE3) chromosome.

For this purpose pKD46 with the protocol as described by Datsenko and Wanner 2000, with some alterations was utilized. The constructs as described above were made and amplified using SOEing (section 2.1.3) and Gibson Assembly (section 2.1.4). Bacterial cells transformed with pKD46 were grown over night at 30 °C in 50 ml LB and 100 µg/ml ampicillin. The overnight culture was then diluted 1:100 in 50 ml fresh LB, 100 µg/ml ampicillin and 1 mM L-arabinose, and incubated at 30 °C. At OD_{600}=0.6 cells were collected and made electro-competent (section 2.2.4). After addition of 0.5 µg of one of the double stranded constructs, 50 µl cells were transformed using electroporation (section 2.2.4). After transformation, cells were recovered for 1 hour in 1 ml LB with 10 mM $MgSO_4$ and 1 mM L-arabinose. Finally, the cells were plated on LB agar with kanamycin, and grown over night at 37 °C. Growing the transformed cells at this temperature resulted in loss of pKD46.

pSIM plasmids from Datta *et al*., 2006 were utilized in addition to pKD46 (Miche, 2010). This is a collection of plasmids containing the λ red recombination genes and different antibiotic resistance genes. The difference between these and pKD46 is that, in the pSIM plasmids, the recombination genes are under the native λ red phage control (heat-sensitive repressor, section 2.1.2), while expression from pKD46 is induced with L-arabinose. Datta *et al*., 2006 report a 10-fold higher efficiency using pSIMs compared to pKD119, a derivative of pKD46.

The protocol utilized was based on Sharan *et al.*, 2009. *E. coli* BL21 Gold (DE3) was transformed with a pSIM plasmid, and grown with the appropriate antibiotic over night at 30 °C. A colony was inoculated in fresh LB and antibiotic and grown to an OD_{600} of 0.5 at 32 °C. Half the culture was transferred to a new flask, and manually shaken in a water bath at 42 °C for 15 minutes to induce λ red expression. After induction, the culture was cooled on ice, made electro-competent (section 2.2.4) and one of the linear dsDNA constructs was introduced to the cells by electroporation (section 2.2.4).

Removal of the kanamycin cassette from BL21 Gold (DE3) after λ red recombination

The protocol for excising the kanamycin cassette from the *E. coli* genome after introducing it with λ red recombination is based on Cherepanov and Wackernagel, 1995. Recombinant cells harboring the kanamycin resistance cassette were transformed with pCP20 and grown on LB plates at 30 °C over night. During this time, the Flp recombinase removed the kanamycin cassette from the genome (section 1.2.3). Kanamycin sensitive clones were identified by streaking each colony on a kanamycin plate and a LB plate, and identify colonies that grew only on the LB plate. The pCP20 plasmid was lost from the cells by growth at 42 °C. Plasmid loss was verified by identifying ampicillin sensitive clones as described above.

2.7 Statistics

2.7.1 Cells corresponding to an OD_{600} of 0.6 for selective detergent treatment

To collect cells corresponding to an OD_{600} of 0.6 in a final volume of 20 ml for selective detergent treatment of the membrane fractions, the following calculations were used.

$$\boldsymbol{n} = c_2 * V_2 = 0.6 * 20\ ml = \mathbf{12}\ \boldsymbol{moles}$$

$$\boldsymbol{V_1} = \frac{n}{c_1} = \frac{\mathbf{12}}{\boldsymbol{c_1}}$$

Where n corresponds to the number of cells (moles), c_2 is the final cell concentration, V_2 is the final volume (ml), V_1 is the volume of cell culture to be collected (ml), and c_1 is the culture concentration (measured in OD_{600}). V_1 is the unknown factor, calculated with n and c_1.

2.7.2 Calculation of the percentage of the total fluorescence in a membrane fraction

To display the fluorescence results obtained after membrane separations, the percentage of the total fluorescence recovered in the two membrane fractions was calculated as shown below.

$$Percentage\ of\ total\ fluorescence\ in\ a\ membrane\ fraction = \left(\frac{X}{Y}\right) * 100$$

Where X refers to the fluorescence in a membrane fraction, and Y is the total fluorescence.

2.7.3 Mean and standard deviation

The graphs in the results display the mean of N experiments calculated as shown below.

$$\bar{X} = \frac{\sum X}{N}$$

Where $\overline{X}$ refers to the mean of the measurements, X is the individual measurements, and N is the number of experiments.

The standard deviations (SD) displayed in the results were calculated as shown below.

$$SD = \sqrt{\frac{\sum\left(X - \overline{X}\right)^2}{N - 1}}$$

Where X refers to the individual measurements, $\overline{X}$ is the mean of the measurements, and N is the number of experiments.

2.8 Protein structure visualization

Protein structures as seen in the introduction were uploaded from the Protein Data Base and adjusted with PyMOL.

3 Results

The aims of this project were to (i) create *E. coli* strains expressing fluorescent labels targeted to the two membranes, and (ii) evaluate the two membrane separation techniques described above based on the purity of the two fractions and the simplicity of the methods. The project was initiated by targeting the fluorescent biomarkers to the desired membranes by fusing the genes encoding a fluorescent protein and a membrane protein or an artificial signal sequence. These initial experiments were performed by expressing the fusion genes from a plasmid. By expressing the six fusion genes and separating the membranes with the selective detergent treatment, the four most promising constructs were chosen for further experiments based on the separation results. In the subsequent experiments, the second separation technique, separation with density gradient centrifugation, was used. This technique is more time consuming, but results in a better separation (Thein *et al.*, 2010). In the last part of the project, the two constructs with most potential to function as fluorescent membrane labels were to be cloned into the genome of *E. coli* BL21 Gold (DE3). It was also attempted to combine the two fusion genes in a plasmid and co-express these before separating the membranes to look at the localization.

3.1 The absolute fluorescence of the control compared to the fluorescent proteins

Figure 10 displays the absolute fluorescent intensities of the lysates after induction of expression from pACYCDuet-1 containing the fluorescent labels. The negative control experiments were performed with BL21 Gold (DE3) transformed with an empty pACYCDuet-1. The figure shows that there was a minimal amount of autofluorescence (section 1.2.1) in the control lysate. This indicates that the fluorescence measured when the constructs were present was signal from these, and not from autofluorescence. Further experiments to verify the separation of the two membranes were also performed with the control fractions after membrane separation. These results can be found in section 3.4.

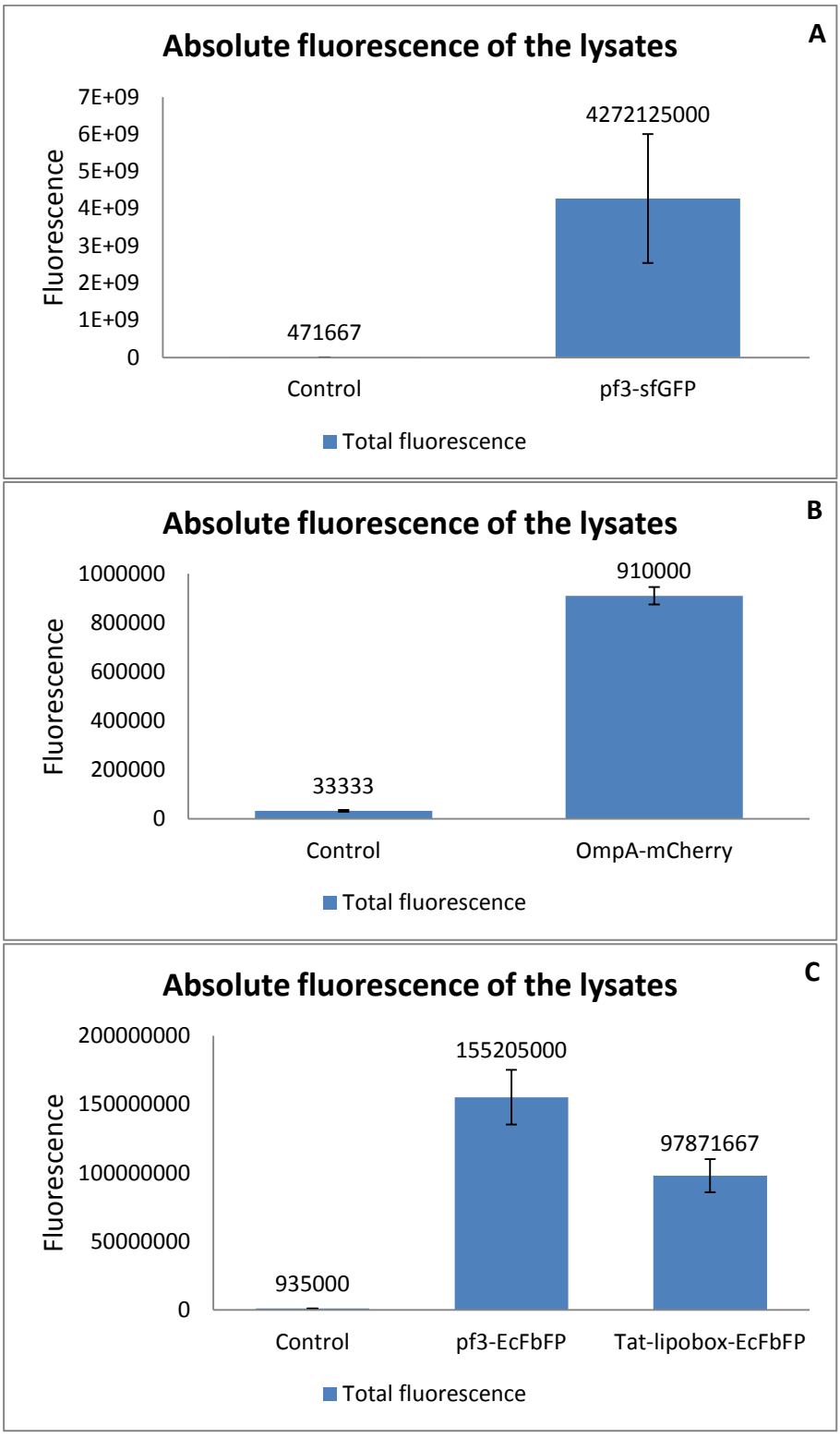

Figure 10: The absolute fluorescence of the lysates after autoinduction and cellular lysis. The total fluorescence measured of the lysates from the induced cultures after transformation with an empty pACYCDuet-1(control) or pACYCDuet-1 containing the fluorescent labels. The graph displays the mean and SD of N=3 experiments (section 2.7.3). The control values in the three graphs are the fluorescence measured from the same experiments, but at the appropriate excitation and emission wavelengths for comparison to the fluorescent protein in question. A) 485 nm (excitation), 510 nm (emission), B) 587 nm (excitation), 612 nm (emission), C) 450 nm (excitation), 495 nm (emission).

3.2 Initial experiments to test the biomarkers for fluorescence and localization

In the first part of the project, the membrane separation technique based on selective detergent treatment was chosen due to its simplicity, small scale, and speed. The technique was utilized to assess the quality of the fluorescent membrane constructs created for the project. This assessment was performed by separating the membranes after fluorescent label expression and transport to the intended membrane. The results were obtained by measuring the fluorescence of the cell lysate and the two membrane fractions, hence acquiring the percentage of the total fluorescence that ended up in the two membrane fractions after separation.

3.2.1 Partioning of fluorescent probes to different membranes by selective detergent solubilization

These fluorescence results were obtained by growing BL21 Gold (DE3) transformed with pACYCDuet-1 with the fusion gene in question at 26 °C for 16 hours in autoinduction medium, and separating the membranes using the selective detergent treatment method.

Figure 11 displays the percentage of the total fluorescence found in the two membrane fractions after membrane separation. As seen in the figure, a major part of the total fluorescence measured for the IM constructs was lost during the separation. This was more pronounced for the constructs containing the IM protein Mistic. However, the remaining fluorescence was mostly found in the IM fractions. Looking at the Tat-lipobox-EcFbFP construct, almost all the total fluorescence was lost, and only a minor part was found in the membrane fractions. A marginally higher fluorescence was measured in the IM fraction compared to the OM fraction. As Tat-lipobox-EcFbFP was intended for the OM, this indicates a failed delivery of EcFbFP to the OM using the artificial Tat-lipobox signal sequence. When separating the membranes from cells expressing the OmpA-mCherry construct, less fluorescence is lost compared to the other constructs. However, the remaining fluorescence is mostly found in the IM fraction, not in the desired OM fraction.

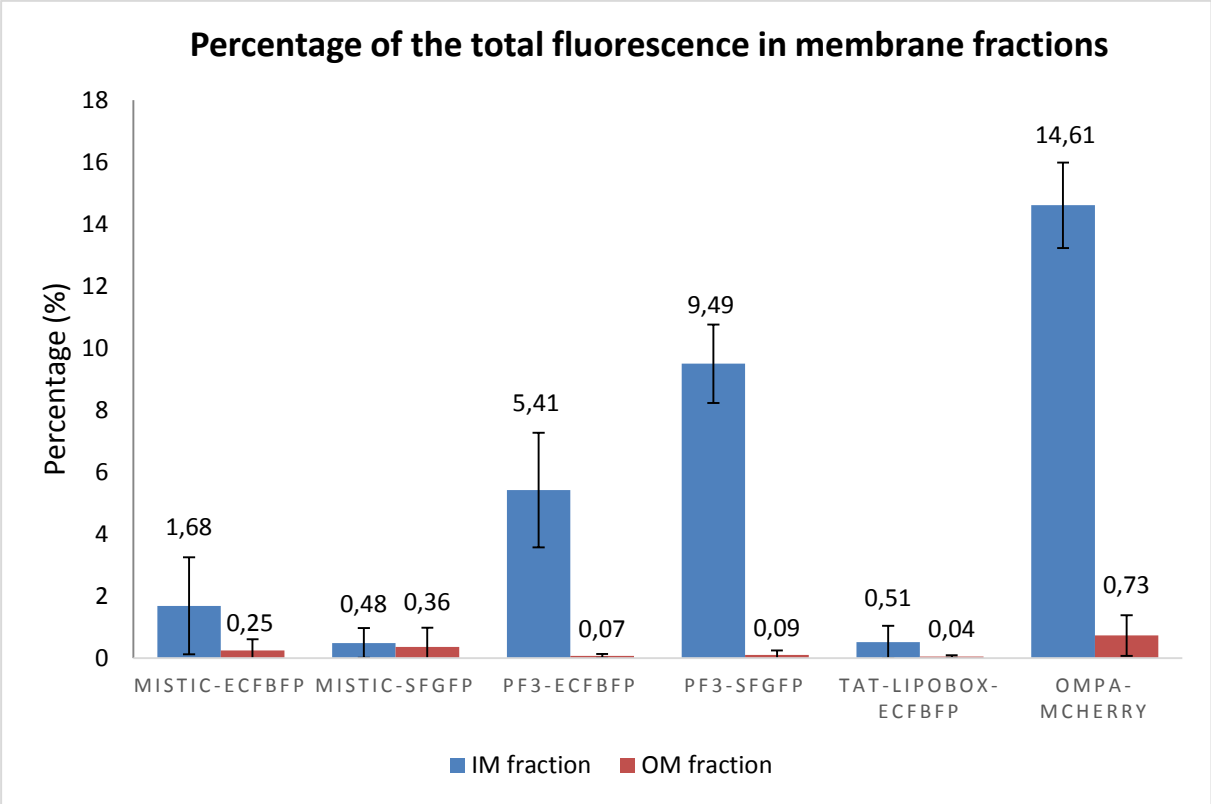

Figure 11: Percentage of the total fluorescence in the membrane fractions. After membrane separation using the selective detergent treatment method, the percentage of the total fluorescence recovered in the two fractions were calculated (section 2.7.2). The IM constructs are Mistic-EcFbFP, Mistic-sfGFP, pf3-EcFbFP, pf3-sfGFP. The outer membrane constructs are Tat-lipobox-EcFbFP and OmpA-mCherry. The graph displays the mean and the SD of N=3 experiments (section 2.7.3).

In the protocol used to obtain the results in Fig. 11, the membranes were pelleted at 15 600 x *g*. However, according to most protocols, a minimum of 100 000 x *g* are required to efficiently pellet membrane vesicles (Thein *et al.*, 2010, Osborn and Munson, 1974). I therefore applied the selective detergent treatment technique on BL21 Gold (DE3) transformed with pACYCDuet-1 with OmpA-mCherry after autoinduction, but with membrane pelleting at 100 000 x *g*. The result can be seen in Figure 12. This did not decrease the loss of total fluorescence, but a larger part of the total fluorescence was now found in the OM fraction.

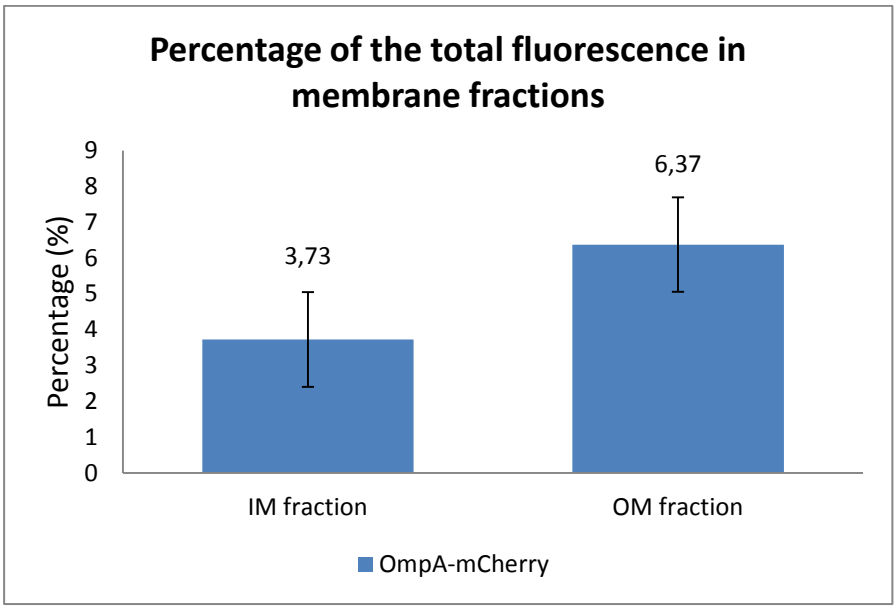

Figure 12: Percentage of the total fluorescence in the membrane fractions (section 2.7.2). Membranes were separated after autoinduction of OmpA-mCherry expression from pACYCDuet-1. The separation technique using a selective detergent was used with an ultracentrifuge at 100 000 x *g* to pellet the membranes. The graph displays the mean and the SD of N=3 experiments (section 2.7.3).

Considering these results, I determined to continue with four constructs, two IM constructs and two OM constructs. The two pf3 constructs were chosen due to the good separation and the smaller loss of total fluorescence compared to the two Mistic constructs. I decided to continue with both OM constructs despite the less promising results obtained for the Tat-lipobox-EcFbFP construct. Further experiments were performed with these four biomarkers.

3.3 Experiments to further verify the localization of the fluorescent membrane labels

3.3.1 Partioning of fluorescent probes to different membranes by density gradient centrifugation

The fluorescence of the membrane fractions was measured as explained in section 3.2, but the membranes were separated with the density gradient centrifugation method. Figure 13 displays the percentage of the total fluorescence found in the two membrane fractions. Looking at the two IM constructs, a major part of the total fluorescence was lost, as was the case with the results obtained with the selective detergent treatment. A small part of the total fluorescence was found in the OM fractions, but the majority of the recovered fluorescence was found in the IM fractions. The Tat-lipobox-EcFbFP construct still lost close to all the

total fluorescence, confirming the results from the selective detergent treatment that this artificial signal sequence was not able to direct EcFbFP to the OM. Very promising results were obtained for the OmpA-mCherry construct. As seen the Fig. 13, approx. 82 % of the total fluorescence was located in the OM fraction. Less than 5 % of the total fluorescence was lost in this separation.

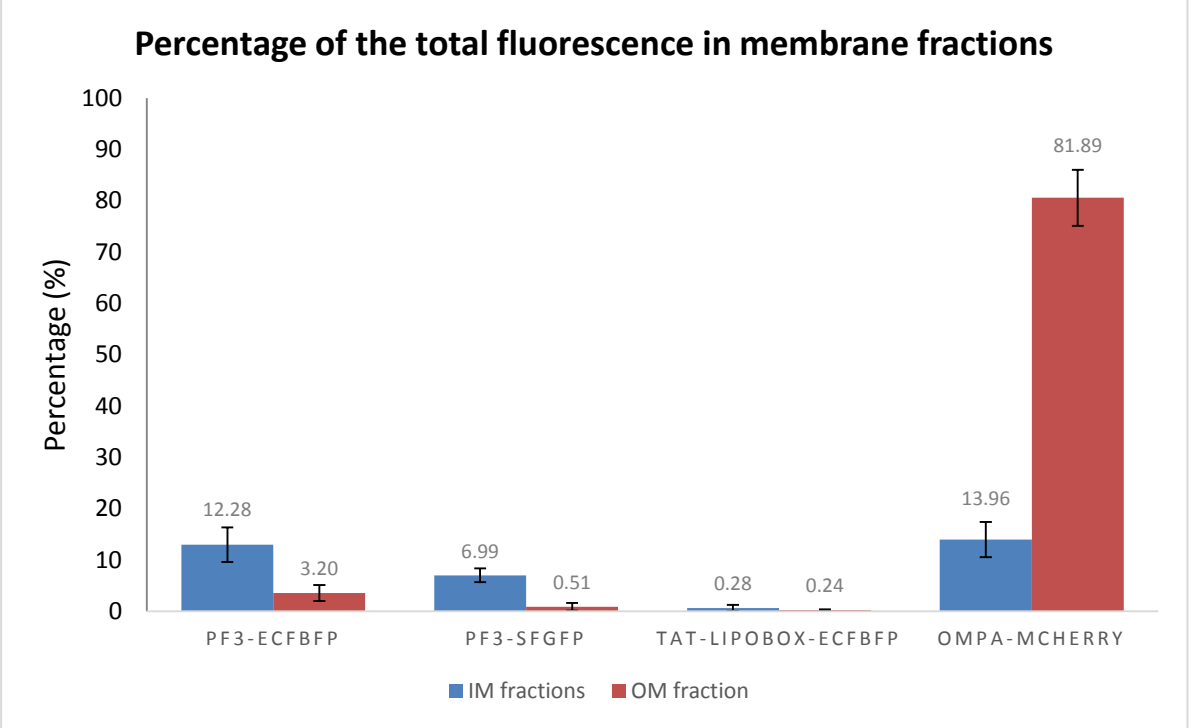

Figure 13: Percentage of the total fluorescence in the membrane fractions. After membrane separation using the density gradient centrifugation method, the percentage of the total fluorescence recovered in the two fractions were calculated (section 2.7.2). The IM constructs are pf3-EcFbFP and pf3-sfGFP. The OM constructs are Tat-lipobox-EcFbFP and OmpA-mCherry. The graph displays the mean and the SD of N=3 experiments (section 2.7.3).

The close to total loss of fluorescence after membrane separation of membranes from bacteria expressing the Tat-lipobox-EcFbFP construct made me take a closer look at the construct. It turned out that close to 53 % of the total fluorescence was found in the supernatant obtained after pelleting the membranes. This supernatant contains both the cytosolic and the periplasmic fractions.

Considering these results, pf3-sfGFP and OmpA-mCherry were chosen as the constructs to be transferred to the *E. coli* genome.

3.3.2 Sucrose gradients

Figure 14 shows the membranes separated in sucrose gradients. The IM has a lower density compared to the OM and can be seen as the higher band. The amount of membrane loaded on the first four gradients was from 250 ml autoinduction culture. Loading this amount of membrane from cells expressing the pf3-sfGFP construct overloads the gradient, making it difficult to distinguish the two membrane bands. In the far right gradient, membrane from 1/8 of a 500 ml autoinduction culture was loaded. This seems to be the smallest amount possible to load. One can just make out the lower band. The middle band is a mixed one, and was discarded (Thein *et al*., 2010). The figure displays a nice separation of the membranes with distinguishable bands, and a minimal amount of the mixed bands. The placement of the bands in the experiments where fluorescent proteins are expressed coincides with the bands in the control experiment. The gradient showing the separation of membranes with OmpA-mCherry is particularly nice, with the OM band seen as red.

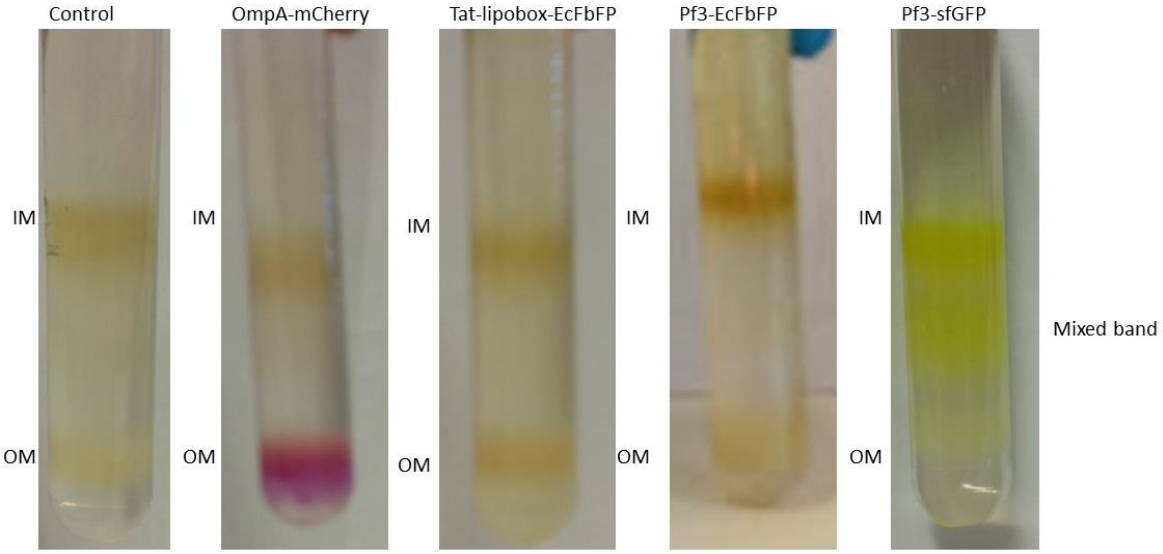

Figure 14: Sucrose gradients after membrane separation by density gradient centrifugation. Sucrose gradients of (from left) the control, OmpA-mCherry, Tat-lipobox-EcFbFP, pf3-EcFbFP, and pf3-sfGFP. The IM, OM and mixed bands are indicated.

3.4 Experiments for additional verification of membrane separations

As mentioned in the introduction, section 1, there are several ways to confirm the separation of the inner and the outer membranes. In addition to the fluorescence results, we wanted to verify the membrane separations by silver staining SDS-PAGE gels to look at the LPS content

of the two fractions, performing a Western blot using an antibody binding the outer membrane protein OmpX, and measuring the activity of the IM enzyme NADH oxidase.

3.4.1 Silver staining of SDS-PAGE gels

Silver staining is a sensitive technique and only a small amount of sample is required for visualization. 0.8-1 µl of the membrane fractions were run in a polyacrylamide gel as described in section 2.4, and the gel was silver stained (section 2.4.2). The result of silver staining of the fractions obtained from the control and the two IM and two OM constructs chosen after the first round of membrane separation can be seen in Figure 15. Silver staining was mainly utilized to visualize LPS in in the membrane fractions, which can be seen as dark stains at the size of ~10 kDa. One can see a difference in the amount of LPS in the two fractions, which is more prominent for the four constructs. Other bands to note in this figure are the two bands at around 40 kDa. The size of these correspond to the outer membrane porins OmpC (PDB: 2J1N) and OmpF (PDB: 4JFB). In both figures, these two bands have a higher intensity in the OM fractions compared to the IM fractions. However, they can be seen in both fractions, indicating that the separation using a selective detergent is not complete.

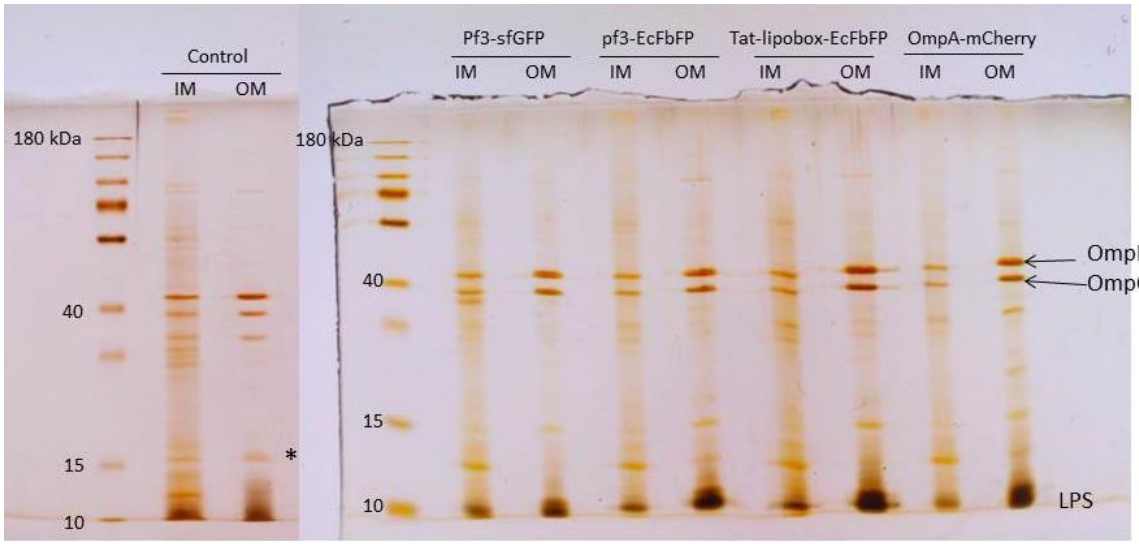

Figure 15: Silver stained SDS-PAGE gels of the IM and OM fractions of the control and the four constructs separated with the selective detergent treatment. The bands representing the OM porins OmpF and OmpC and the LPS are labelled.

Figure 16 displays the silver stained SDS-PAGE gels of the fractions obtained from the control and the four constructs, respectively, after separation of the membranes with density gradient centrifugation. Comparing these to the silver stained gels of the fractions obtained

through selective detergent treatment (Figure 15), several new bands appear in the density gradient centrifugation fractions. This is partly due to the larger scale these experiments were performed at, resulting in fractions with higher protein content. In the gels in Fig. 16, one can also see the two outer membrane porins at approx. 40 kDa as more intense in the OM fraction. Another detail to notice is the LPS content at ~10 kDa, which is notably higher in the OM fractions compared to the IM fractions. These results show the improved separation when using density gradient centrifugation compared to the selective detergent treatment.

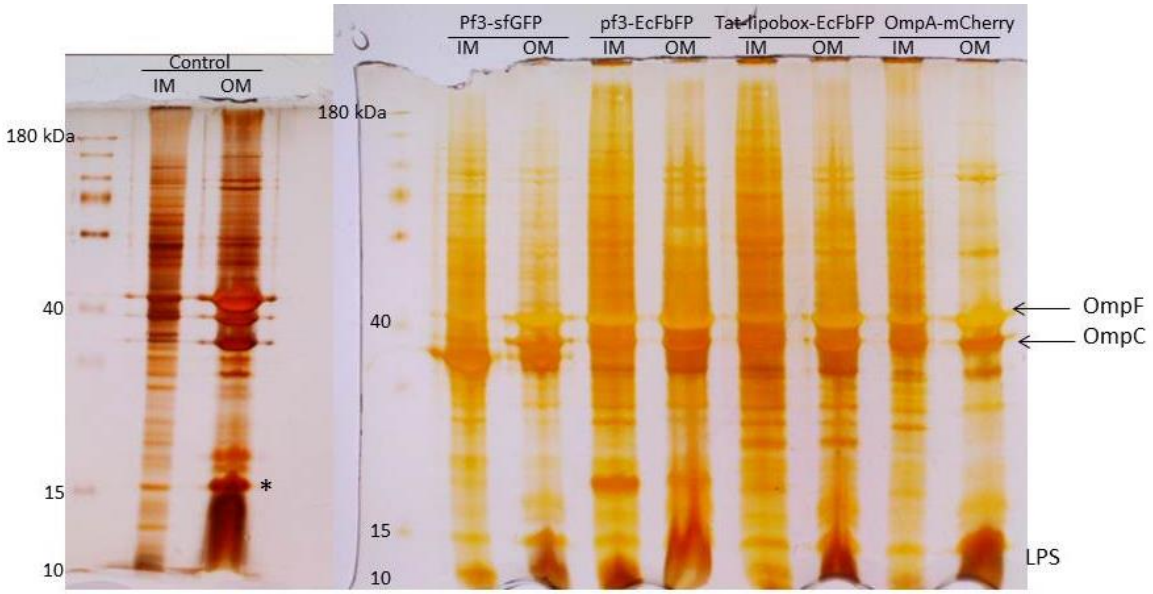

Figure 16: Silver stained SDS-PAGE gels of the fractions after density gradient centrifugation of the control and the four constructs. The bands representing the OM porins OmpF and OmpC and the LPS are labelled.

3.4.2 Western blot

Figure 17 displays the Western blot of the inner and outer membrane fractions after membrane separations of the control probed with an anti-OmpX antibody. OmpX (PDB: 1Q9G) has a size of approx. 16 kDa, and can be seen as the intense bands at its native size. Weak bands can be seen at approx. 40 kDa and 100 kDa. The band at 100 kDa is only visible in the OM fraction after density gradient centrifugation. These larger bands might be OmpX that has escaped denaturing, as β-barrels are very stable and difficult to denature even with SDS. In the native form, proteins will run at a different size in SDS-PAGE gels. The larger bands can also be OmpX multimers that have escaped denaturation.

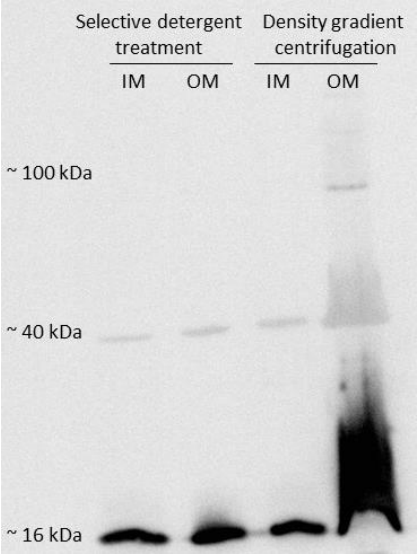

Figure 17: Western blot stained with anti-OmpX. The fractions run on the gel are the IM and OM of the control obtained through the two separation techniques.

It is difficult to see the difference between the intensity of the darkest bands in the Western blot. Comparing the blot with the silver stained gels of the controls (Figures 15 and 16), the band at approx. 16 kDa (labeled with *) is visibly weaker in the IM fractions compared to the OM fractions. But in both cases, OmpX can be found in both fractions, again proving the difficulties in obtaining a pure membrane fraction.

3.4.3 NADH oxidase assay

Figure 18 displays the result of the NADH oxidase assay of the control fractions separated with density gradient centrifugation. Due to time limitations, no attempt was made to optimize the assay. The protocol called for 0.2 units/ml of enzyme, which is difficult to accommodate as the enzyme was not purified, but in the purified membrane. To measure the NAHD activity, a large amount of the membrane fractions were added to the reaction mix before measuring the decrease in absorbance at 340 nm. The system was most likely overloaded with protein, hence the poor result. Looking at the figure, there is a small difference between the IM and the OM fractions. The slope of the IM fraction is steeper compared to the OM fraction, suggesting a higher NADH oxidase activity here. There is a slope in the control measurements as well. These measurements should have been more or less without a slope, at the least to a smaller extent than the IM fraction.

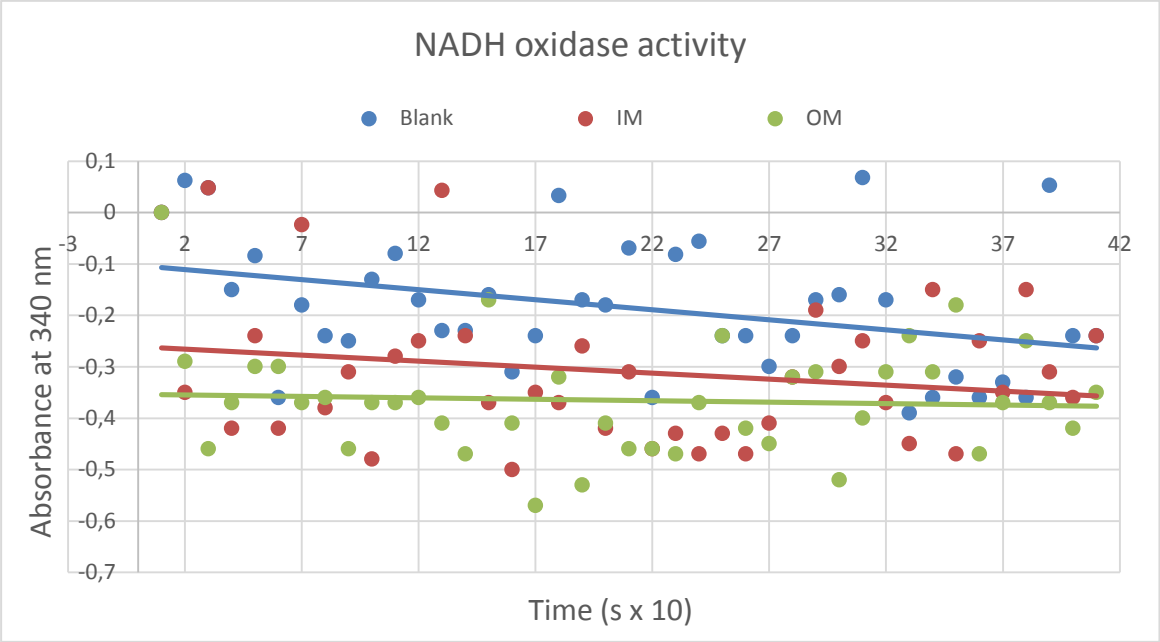

Figure 18: NADH oxidase activity assay of the two fractions after density gradient centrifugation of the control. N=1.

3.5 Improvement of the density gradient centrifugation method

3.5.1 Inclusion bodies

During cell lysis of bacterial cells expressing the fluorescent biomarkers, the lysate appeared milky (Figure 19). Pelleted membranes have a gel-like, translucent appearance, but I also observed a white substance in the bottom of the tubes after the membranes were pelleted. The milky lysate and the white pellet are consistent with inclusion body formation, an event where overexpression can cause aggregation of proteins in the cytosol to a condensed heap consisting mostly of β-structures (Carrió *et al.*, 2005). I therefore attempted to reduce this formation during protein expression, and to remove the inclusion bodies from the membrane fractions. In the first attempt to improve the separation, the expression of pf3-sfGFP was not induced or induced with low levels of IPTG in place of autoinduction. I chose to test one uninduced culture to investigate the bleed-through from the plasmid. To the induced cultures, 0.25 mM or 0.5 mM IPTG was added (section 2.2.5), and the membranes from the three cultures were separated with the density gradient centrifugation method.

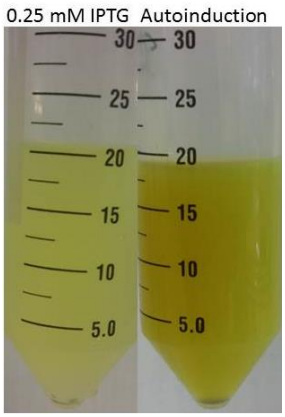

Figure 19: Cell lysates of BL21 Gold (DE3) transformed with pACYCDuet-1 with pf3-sfGFP and induced with 0.25 mM IPTG (left) or autoinduced with ZYP-5052 (right). There is a clear difference between the two lysates: the milkiness of the lysate from the autoinduced culture is presumably due to inclusion bodies.

Figure 20 displays the percentage of the total fluorescence found in the membrane fractions after no induction or low levels of IPTG induction, and membrane separation using density gradient centrifugation. The percentage yield in the two membrane fractions has increased compared to the results from the autoinduction (Figure 13, section 3.3.1). We can conclude that one of the reasons for loss of total fluorescence was inclusion body formation. The figure makes it evident that there is a bleed-through of expression of the T7 RNA polymerase from the bacterial genome (0 mM IPTG), and hence expression from the plasmid. In the bleed through experiment, a higher amount of the fluorescence is found in the OM fraction, not in the desired IM fraction. More fluorescence was recovered with IPTG induction compared to the autoinduction (Figure 13), but this increase can be seen in the OM fraction, not in the IM fraction. The high SD, particularly in the bleed through experiments indicates that the experiment should be repeated.

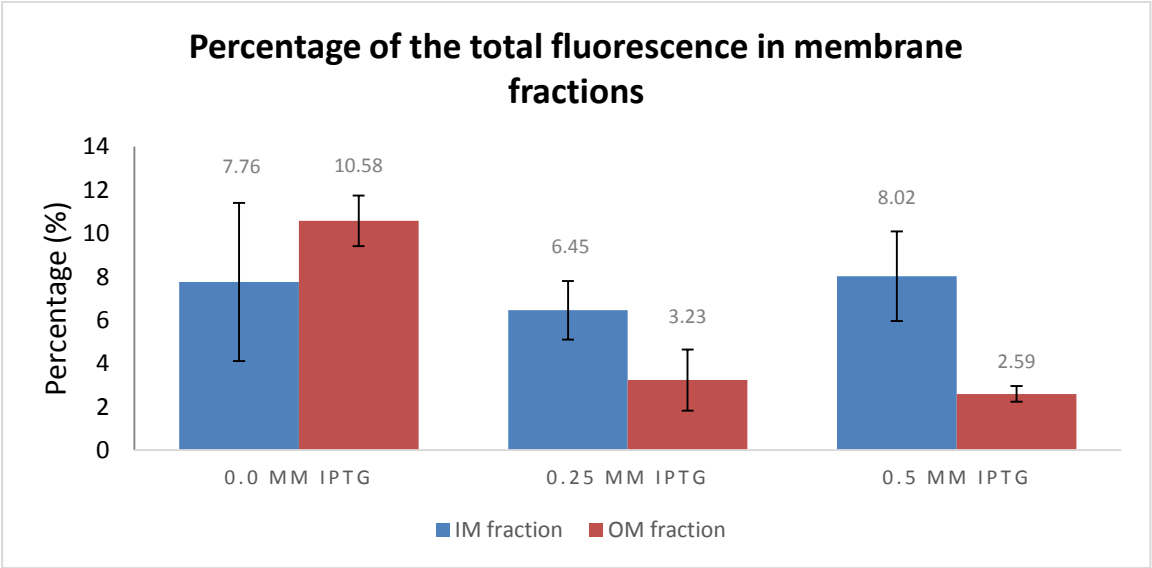

Figure 20: Percentage of total fluorescence in membrane fractions (section 2.7.2). The IM and the OM fractions were obtained with density gradient centrifugation of uninduced cells and cells induced with 0.25 or 0.50 mM IPTG for pf3-sfGFP expression. The graph displays the mean and the SD of N=2 experiments (section 2.7.3).

The silver-stained gel of membranes isolated from bacteria expressing pf3-sfGFP and induced with different IPTG concentrations can be seen in Figure 21. The reason for the higher amount of protein in the 0 mM IPTG lanes is most likely because these bacteria grew better compared to the induced cultures. The LPS content of the lanes confirm the quality of the separation.

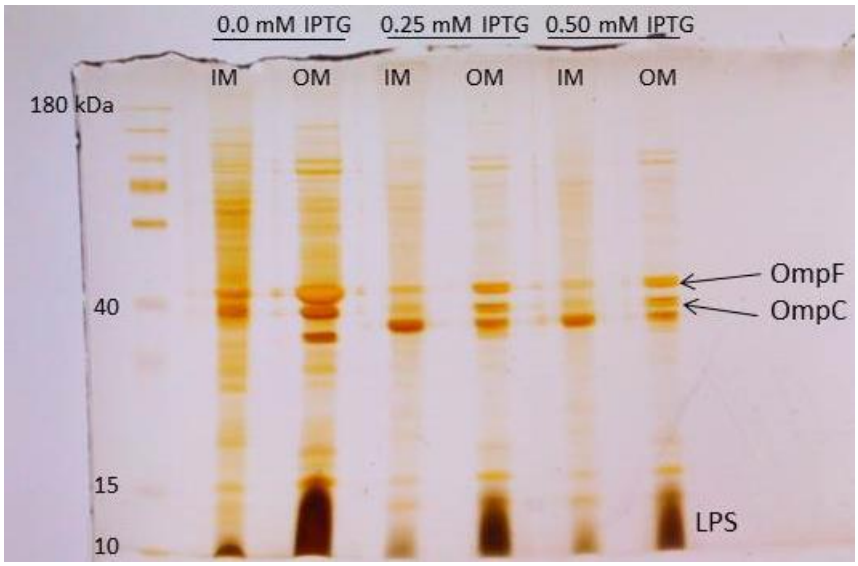

Figure 21: Silver stained SDS-PAGE gel of the membrane fractions after density gradient centrifugation of cells expressing pf3-sfGFP. The cell cultures were uninduced or induced with 0.25 mM or 0.50 mM IPTG.

3.5.2 Peptidoglycan treatment and membrane washing

As the IPTG induction did not seem to increase the transport of the fluorescent labels to the appropriate membrane, a second attempt to improve the separation was made by treating the lysate with lysozyme and washing the membranes with a high salt buffer. In addition to spanning the membrane, proteins may also be anchored in the periplasm. By treating the lysate with lysozyme, we wanted to remove residual peptidoglycan that might cause membrane vesicles to stick together. The high salt buffer was used to reduce unspecific binding and hopefully reduce the amount of vesicles ending up in the mixed band. The membrane fractions were separated using the density gradient centrifugation protocol described in section 2.3.2. Figure 22 shows the result.

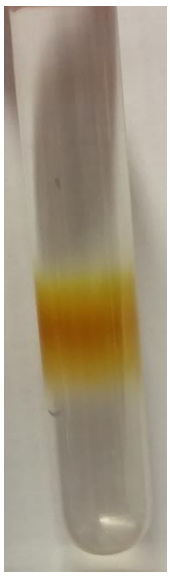

Figure 22: Result of density gradient centrifugation after lysozyme and high salt buffer treatment. There was no proper separation of the two membranes.

Only one band could be seen in the gradient, and this method was discarded. In the future, it would be interesting to perform the washing steps using a low ionic strength buffer and investigate whether this improves the separation or decreases the amount of the mixed band.

3.6 λ Red Recombination

λ red recombination was chosen as a method for the transfer OmpA-mCherry and pf3-sfGFP into the genome of *E. coli* BL21 Gold (DE3) and BL21 (DE3) ΔABCF. Constructs containing a promoter, a fusion gene, a terminator, and a kanamycin cassette for selection of recombinant clones were made using Gibson Assembly (section 2.1.4) or SOEing (section 2.1.3). The three plasmids described in section 2.7 containing the λ red recombination genes were extensively tested by changing induction time, inducer concentration and at what density cells were collected and made electro-competent. Even after growth over several days on plates, no positive colonies were obtained. More optimization or a different method is necessary to finish the project.

Due to the lack of positive recombinants, the outer membrane label OmpA-mCherry was attempted to be cloned into the second multiple cloning site of pACYCDuet-1 already containing the IM label pf3-sfGFP in the first multiple cloning site. Expression would then be induced with autoinduction and the membranes separated using density gradient centrifugation. This was not achieved due to problems when opening pACYCDuet-1 at the second multiple cloning site for Gibson Assembly. As the plasmid is designed to contain the same ribosome binding site at both cloning sites, there was unspecific binding of the primers during PCR, leading to several products with different sizes after the PCR reactions.

4 Discussion

The aim of this project was to create stable *E. coli* strains expressing fluorescent biomarkers for simple verification of the fractionation of the Gram-negative bacterial membranes. Furthermore, we wanted to utilize and compare two commonly used membrane separation techniques to verify the translocation of these fluorescent biomarkers to their respective membranes. The fluorescent biomarkers were made by fusing the gene encoding a fluorescent protein to a gene encoding a known membrane protein or an artificial signal sequence. The six constructs, two intended for the OM and four intended for the IM, were expressed separately from a plasmid and tested for their localization with the first membrane separation technique, the selective detergent treatment. Based on these results, two OM and two IM constructs were chosen for further testing and evaluation of the next membrane separation technique, the density gradient centrifugation. Finally, the two constructs OmpA-mCherry and pf3-sfGFP were chosen to be transferred to the *E. coli* genome using λ red recombination. This part of the project was not finalized due to time limitations and difficulties with the chosen method.

4.1 The quality of the fluorescent labels

The control fractions obtained with the two membrane separation techniques show some fluorescence when investigated with the plate reader (Figure 10, section 3.1). This is autofluorescence due to cellular compounds such as NADH and flavoproteins (section 1.2.1). Compared to the detected fluorescence when measuring the lysates containing fluorescent proteins, the fluorescence values of the controls are sufficiently low to consider them insignificant.

4.1.1 Inclusion body formation as an explanation for loss of fluorescence

All constructs, except the OM construct Tat-lipobox-EcFbFP, seemed to be translocated to the intended membrane (Figure 11, section 3.2.1 and figure 13, section 3.3.1). The loss of total fluorescence was partly due to inclusion body formation, which can be corrected for by a reduced protein expression. This is achieved by lowering the induction time, reducing the inducer concentration, growing the cells at a lower temperature, or, for some proteins, grow the cells in an enriched growth medium (Moore *et al*., 1993). Inclusion body formation was

particularly evident for the pf3-sfGFP construct. This might be due to the formation of biologically active inclusion bodies (section 1.2.1). Huang *et al*., 2013 found that the GFP moiety has the ability to form loose aggregates during folding, but remain fluorescently active. This indicates that even though the total fluorescence in the cell is high, only a small fraction is transported to the intended membrane and the rest is left in the cytosol. As the fluorescent strains made in this project are to be used for protein expression of other membrane proteins, it would be a disadvantage to have formation of inclusion bodies in the cytosol. These may interfere with the folding and transport of the protein co-expressed with the fluorescent biomarkers.

Several publications discuss the attempt to separate the two membranes of Gram-negative bacteria using different techniques, including density gradient centrifugation. When using this method, several studies report a 3rd mixed band that is discarded *(*Osborn *et al.,* 1972, Thein *et al*., 2010). Osborn *et al.,* 1972 reports that this band can contain up to 15 % of the total membrane protein. This could also account for some of the loss of fluorescence after membrane separation.

These results and observations lead to the conclusion that a low expression of fluorescent proteins will result in the best fluorescent strains for the purpose they are intended. Three promoters were chosen to be cloned into the *E. coli* genome with the fusion genes, two constitutive and one inducible (section 1.2.3). When the time comes to test these clones, it would be beneficial to grow the cells at a low temperature to ensure reduced expression. When utilizing the inducible promoter, a small amount of inducer will be sufficient. The constitutive promoters chosen were one with high strength and one with reduced strength. Based on my results, I assume that the promoter with low strength will be more successful. As the goal of the protein expression is to label the membranes with fluorescent biomarkers, not high protein yields, it is not necessary to have a high amount of fluorescent proteins in the membranes. As long as the fluorescence can be detected, a lower amount will suffice for specific membrane labelling while avoiding problems associated with overexpression of the fluorescent construct, such as inclusion body formation and membrane mistargeting. When transferring the fluorescent proteins to the *E. coli* genome, the cell will contain one copy of the gene instead of several copies that comes with the expression from a plasmid. This will reduce the number of recombinant proteins in the cell, hence reducing inclusion body formation and improve transport to the intended membrane.

The OM construct chosen for the final strains was OmpA-mCherry. Inclusion body formation was not a problem when expressing this fusion protein as the major part of the fluorescence was recovered in the desired membrane fraction (Figure 13, section 3.3.1). A reduced expression of this fluorescent biomarker in the final *E. coli* strains will be beneficial to make room for other OM proteins.

4.1.2 Labeling the outer membrane with the artificial Tat-lipobox sequence

The artificial Tat-lipobox signal sequence did not direct EcFbFP to the OM as expected. Looking at the fluorescence results (Figure 11, section 3.2.1 and figure 13, section 3.3.1), there seemed to be no transport to any membrane. The lipobox used in the project was in the form of L-A-G-C-D, with the cleavage site between G and C. As it turns out, a D in position 2 (adjacent to the acetylated C in position 1) in a lipoprotein leads to retention of this protein in the IM (Lol avoidance signal, section 1.1.2), while a S at the same position leads to transport to the OM (Yamaguchi *et al*., 1988). The strength of this retention signal is increased when D, glutamatic acid, or glutamine is in position 3 (Terada *et al*., 2001). Even though the residue at position 3 in the Tat-lipobox-EcFbFP construct was not any of these amino acids, the D at position 2 may have caused a sufficient retention signal to inhibit the transport of Tat-lipobox-EcFbFP to the OM. However, if this construct was retained in the IM, a more significant fluorescent signal would have been detected here.

Because 53 % of the total fluorescence was found in the supernatant after membrane pelleting (section 3.3.1), it is possible that another aspect of the artificial signal sequence is blocking the translocation to the desired membrane. As the periplasm was not removed from the cells before cellular lysis, the supernatant after pelleting the membranes will be a mixture of the cytosol and the periplasm. The two possible fates for the protein are (1) that there is no export to the periplasm, leaving the fluorescent protein it in the cytosol, or (2) there is transport across the IM, but no acetylation of the lipobox. This would lead to release of the fluorescent protein into the periplasm. As the Tat signal peptide has been successfully utilized by others (Blaudeck *et al*., 2001), and studies show lipoproteins with the intact lipobox as substrates for the Tat translocase (Stefanie *et al*., 2010), it is difficult to pinpoint why the Tat-lipobox-EcFbFP construct was not transported to the OM. It has been hypothesized though, that there is a "folding quality control" of proteins before they are transported across the membrane by

the Tat translocase (DeLisa *et al*., 2003). If EcFbFP is slow folding or contain features the translocase complex does not recognize, this might be the reason for the lack of transport.

4.1.3 Utilizing Mistic as a tool to direct proteins to the inner membrane

The fusion of fluorescent proteins to the integral inner membrane protein Mistic did not label the IM with the same efficiency as when pf3 was utilized. Efficient translocation of Mistic into the IM has been reported (Kefala *et al*., 2007), but this system did not seem to be equally applicable for our purpose. It is unknown how Mistic is integrated into the IM, and it is hence difficult to speculate as to what this inefficient translocation is caused by. It may be that the fusion between Mistic and sfGFP/EcFbFP interferes with the translocation or the folding of the protein, leading to inefficient translocation to the IM. The peptide linker, GSGS, which was used as a linker between all fusion proteins, might have to be elongated or changed to allow proper folding.

There was a higher spread in the results where EcFbFP was used as the fluorescent label in this project, including where it is fused with Mistic. This indicates that the translocation efficiency of EcFbFP is more variable compared to the other fluorescent markers. This might be due to inefficient folding or transport of EcFbFP. As both EcFbFP and Mistic are relatively recently discovered native *B. subtilis* proteins, they might have unforeseen problems when expressed in *E. coli*.

4.2 Quality of the membrane separation techniques

The results display a clear difference between the qualities of the membrane separation techniques. This is particularly evident in the fluorescence results. When separating the membranes with the selective detergent treatment method, the results show contaminations in the two fractions. Looking at OmpA-mCherry, a higher percentage is found in the IM after protein expression compared to the OM with this method (Figure 11, section 3.2.1). The fluorescence results after membrane separation using density gradient centrifugation, however, confirms the localization of OmpA-mCherry to the OM (Figure 13, section 3.3.1). These results prove that the selective detergent treatment is a method for enrichment of OM proteins, but a significant amount of the OM is solubilized by lauroyl sarcosine, which results

in an IM fraction containing a large amount of OM contaminants. The fluorescence result for the other constructs, such as pf3-sfGFP, shows that the OM fraction obtained with the selective detergent treatment contains less contamination from the IM fraction.

Previous studies have also speculated that the treatment of an OM fraction with lauroyl sarcosine may cause the solubilization of some OM proteins (Chopra and Shales, 1980). Chopra and Shales, 1980 tested for IM enzyme activity in OM fractions before and after lauroyl sarcosine treatment, and found that the activity of these IM enzymes did not change after treatment. The activity was low, but this confirms a contamination of an IM enzyme in the OM fraction and proves that lauroyl sarcosine does not completely solubilize the IM. The 2D SDS-PAGE performed in the same study showed that 1.2 % of proteins in the OM fraction were lost due to the detergent treatment. This can explain the contamination of OM proteins in my IM fractions, and *vice versa*.

The differences between the two methods can also be seen in the silver-stained gels (Figures 15 and 16, section 3.4.1). The fractions from the selective detergent treatment contain less protein when compared to the same results from the density gradient centrifugation. The most visible difference between the two is in the range of the proteins with a size above 40 kDa. These are mostly missing in the samples from the selective detergent treated fractions. One reason for the difference is the larger scale of the cultures used for density gradient centrifugation, creating a higher concentration of proteins in these fractions. However, as less of the fractions obtained with the density gradient centrifugation were loaded on the gels, the scale difference between the two methods cannot be the only reason for the difference in the banding pattern. There are contaminants in both membrane fractions after membrane separation using both techniques. The most visible difference between the two methods is the LPS content of the fractions. The silver stained gels show a higher separation of LPS between the two fractions with the density gradient centrifugation compared to the selective detergent treatment.

The Western blot also confirms the contamination problem with both separation methods (Figure 17, section 3.4.2). There was OmpX in all fractions obtained with both methods (bands at ~16 kDa), with more intense bands in the OM fractions. This is more prominent when comparing these bands with the corresponding bands in the silver stained gels (bands in control lanes marked with *, Figures 15 and 16, section 3.4.1). The OM bands at ~16 kDa in

the silver stained gels are more intense compared to the IM bands, but there are definite bands in the IM fractions as well.

The enzyme activity in the NADH oxidase assay was confirmed by a reduction in the absorption at 340 nm (Figure 18, section 3.4.3). NADH absorbs light at this wavelength, and the reduced absorption indicates reduced concentration of NADH and hence an enzyme activity. Due to time limitations, the NADH oxidase assay was not optimized as it should have been. The protocol called for 0.2 units/ml of enzyme, which is difficult to oblige when using a membrane fraction with an unknown protein concentration. A large part of the fraction obtained with density gradient centrifugation was added to the cuvette to initiate the experiment, and this might have overloaded the system. As NADH oxidase activity was found in the OM fraction, it is clear that a complete separation of the two membranes is difficult. However, these preliminary results show a higher activity of the enzyme in the IM fraction.

4.2.1 The steps taken to optimize the membrane separation techniques

Improvement of the selective detergent separation was not tested extensively. It would be interesting to try other detergents for the solubilization step, such as Triton X-100. If the protocol were to be changed to this detergent, it would be important to add Mg^{2+} to protect the OM by conserving its structural integrity. Filip *et al.*, 1973 showed that both membranes are solubilized by Triton X-100, but by adding Mg^{2+}, the OM was protected and a good separation was obtained.

The improvement that was made to the selective detergent protocol was changing the membrane pelleting steps in a tabletop centrifuge at 15 600 x *g* to an ultracentrifugation step at 100 000 x *g*. This did improve the membrane yield, but it did not seem to improve the separation. This was most likely due to the solubilization step, not the centrifugation step, and experimentation with different detergents is required. This method was utilized because it is quick and simple, and adding this ultracentrifuge step complicates the protocol, making it more time consuming. Whether to add this or not depends on the users expectations from the procedure – if an OM enrichment is the goal, no ultracentrifugation is needed. But if a higher yield and a proper separation are intended, ultracentrifugation and experimentation with different detergents and detergent concentrations would be beneficial.

Additional steps were included in the protocol to optimize the density gradient centrifugation, including adding a centrifugation step to rid the solution of inclusion bodies, lysozyme treatment to remove residual peptidoglycan, and washing the membranes with a high salt buffer before loading them onto the gradient to reduce unspecific binding (sections 3.5). Treating the membranes with lysozyme is a logical addition to the protocol as peptidoglycan can make the vesicles sticky, an undesirable trait when separating them. The additional centrifugation step to remove inclusion bodies was mostly important for the pf3-sfGFP construct. When expressing this construct, we clearly had inclusion body formation (section 3.5.1). Removing these made the membranes easier to handle in the subsequent steps.

The washing steps with a high ionic strength buffer were a less fortunate choice of improvement (Figure 22, section 3.5.2). The high salt concentration was intended to reduce unspecific binding between vesicles or between vesicles and peripherally attached proteins. As it turns out, Osborn *et al.*, 1972 found that the washing of the membranes with a high ionic strength buffer will interfere with the separation of the two membranes in a sucrose gradient, resulting in one mixed band. We hypothesize that the salt in the buffer might change with the density of the membrane vesicles, making separation more difficult. Washing the membranes before loading can still be advantageous, though, but with a buffer of low ionic strength. Hopefully, this step will reduce the amount of the mixed band obtained in the sucrose gradient.

4.3 A short comparison of the two separation techniques

The density gradient centrifugation and the selective detergent treatment are large scale and small scale methods, respectively, for the separation of the two membranes of Gram-negative bacteria. A summary of the two techniques can be found in Figure 23. The two membrane separation techniques are highly different. While the selective detergent treatment is quick and easy and can, as discussed, be considered an OM enrichment technique (Thein *et al*., 2010), the density gradient centrifugation requires more skill and precision. It can be considered to be a more complete separation technique where all four compartments of the Gram-negative bacteria, the cytosol, the IM, the periplasm, and the OM, can be isolated if a spheroplasting protocol is added. Which technique to utilize for a project depends on the level of separation one wishes to achieve. When a more complete separation is required, the density

gradient centrifugation method is to be preferred. This protocol can be combined with lysozyme/EDTA treatment or cold osmotic shock treatment to obtain the periplasm as well, leading to a full subfractionation of the four major compartments of a Gram-negative bacterium. If the goal of an experiment is the OM proteins, the selective detergent treatment will suffice.

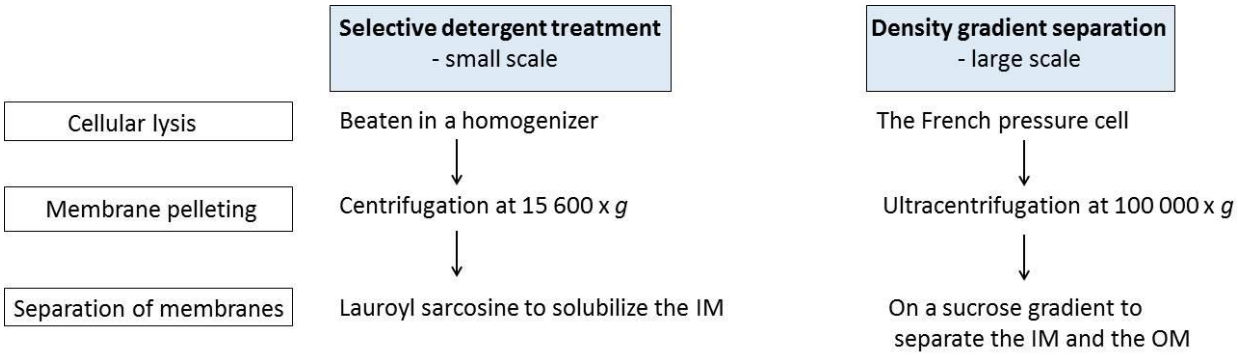

Figure 23: Comparison of the membrane separation methods selective detergent treatment and density gradient centrifugation.

4.4 The generation of *E. coli* strains stably expressing the fluorescent biomarkers

After deciding on one IM and one OM construct for the final fluorescent strains, these were to be transferred into the genome of *E. coli* BL21 Gold (DE3) and BL21 (DE3) ΔABCF. Regrettably, the method chosen for this part of the project was not optimal for BL21 (DE3) derivatives. Other researchers have had troubles with the λ red recombination system using pKD46 (Miche, 2010), and after several unsuccessful tries with this plasmid, I switched to using the pSIM plasmids in place of pKD46. These plasmids supposedly work better due to the natural regulation of the gene expression with a temperature-sensitive repressor instead of the L-arabinose induction in pKD46 and derivatives (Datta *et al*., 2006). We speculated that L-arabinose would not work efficiently in BL21 Gold (DE3) because this strain contains an intact *ara* operon and can therefore metabolize L-arabinose. We hypothesized that the cells would use the L-arabinose added to the culture for induction as a carbon source, hence diminishing the induction efficiency. The pSIM plasmids are induced by shaking the cultures in a water bath at 42 °C. The water bath is required for an efficient heat transfer due to the short induction time – 15 minutes. As the laboratory did not have a water bath shaker, the

induction was performed with manual shaking. This reduces the rpm of this step, which might be one reason for the poor results.

Even though the λ red recombination system for genome editing appears to be a straight forward system, it requires adaption to the strain of interest and a lot of screening of the recombinant clones. In a time-limited project such as this, if the laboratory does not already have optimized protocols for the system, the generation of a recombinant strain may prove to time consuming. If time had been less limiting, other genome editing systems could have been utilized as well, such as the CRISPR/Cas9 system (Hsu *et al*., 2014) or viral transduction (Lennox, 1955).

4.5 Future perspectives

For continuation of this project, the obvious first step would be to finish producing the intended strains either by optimizing the λ red recombination system, or by utilizing another genome editing system. Following the completion of the planned strains with the three different promoters (section 1.2.1), expression of the fluorescent biomarkers and separation of the membranes to confirm the localization, is the logical next step. A nice addition to the project would also be to obtain super-resolution fluorescence microscopy images of the strains, displaying the two fluorescent membranes with a dark periplasm in between (Huang *et al*., 2009). I would also spend some time perfecting the separation methods by experimenting with different growth conditions to reduce inclusion body formation and optimize the translocation to the intended membrane. Different detergents and incubation times to solubilize the inner membrane, washing steps with a low salt buffer of the pelleted membranes, and changing the sucrose concentrations in the density gradient to obtain a better separation of the two membranes could also be tested extensively. It would also be interesting to compare using Triton X-100 and lauroyl sarcosine at the solubilization step, as both detergents are widely used for this purpose.

It is also worth looking at membrane yields with different lysis techniques. Using a French pressure cell is known to give high yield of lysed cells, but the more popular technique when it comes to this step is lysozyme and EDTA treatment for spheroplasting (Osborn *et al*., 1972, Thein *et al*., 2010). This step would allow isolation of the periplasm of the cells as well as the two membranes and the cytosol. After spheroplasting, ultrasonic oscilliation or the French

pressure cell can be used to lyse the cells and create membrane vesicles. For smaller scale experiments, one could compare the yields of the homogenizer and ultrasonic disruption of the cells.

Another interesting aspect would be to look at the constructs for improvement. The aggregation of sfGFP could be solved by changing the linker peptide or change the induction/rate of expression. The evident lack of transport of Tat-lipobox-EcFbFP to either membrane could be investigated by localizing where the fluorescent protein ends up – in the cytosol or in the periplasm, and solve this problem by changing the signal peptide. As mentioned, there is a relatively high spread in the experiments with EcFbFP leading to the hypothesis that this fluorescent protein is difficult to transport to the intended membrane. It would therefore be interesting to use mCherry or sfGFP fused to the improved Tat-lipobox signal sequence and investigate whether this affects the efficiency of translocation to the OM.

5 Conclusion

Labeling the membranes of *E. coli* BL21 Gold (DE3) with fluorescent biomarkers turned out to be a time consuming project. The fusion genes were made using Gibson Assembly, expressed from the plasmid pACYCDuet-1 in *E. coli*, and the localization of the fluorescent proteins extensively tested. Six fluorescent biomarkers were narrowed down to two, the IM marker pf3-sfGFP and the OM marker OmpA-mCherry. The final stage of the project, where the fusion genes were to be transferred into the *E. coli* genome, was not completed during the time at hand.

The second aim, to test the two separation techniques and look at differences between them and the quality of the separations, was completed. The selective detergent treatment is a small scale and quick technique for OM enrichment. However, obtaining an uncontaminated IM fraction with this method is difficult, as the selective detergent lauroyl sarcosine solubilizes parts of the OM as well as the IM. On the other hand, the density gradient centrifugation technique results in a more complete separation, and can be combined with protocols for periplasm isolation to fractionate the four major compartments of the Gram-negative bacterium.

In the future, the *E. coli* stain stably expressing the fluorescent markers has to be completed, and some additional optimization studies of the two techniques should be performed.

References

ANDERSON, C. *Anderson collection: constitutive promoters* [Online]. Available: http://parts.igem.org/Promoters/Catalog/Anderson.

ANGELINI, S., DEITERMANN, S. & KOCH, H. G. 2005. FtsY, the bacterial signal-recognition particle receptor, interacts functionally and physically with the SecYEG translocon. *The European Molecular Biology Organization reports,* 6**,** 476-481.

ARNOLD, T., POYNOR, M., NUSSBERGER, S., LUPAS, A. N. & LINKE, D. 2007. Gene duplication of the eight-stranded β-barrel OmpX produces a functional pore: a scenario for the evolution of transmembrane β-barrels. *Journal of molecular biology,* 366**,** 1174-1184.

BAARS, L., YTTERBERG, A. J., DREW, D., WAGNER, S., THILO, C., VAN WIJK, K. J. & DE GIER, J.-W. 2006. Defining the role of the *Escherichia coli* chaperone SecB using comparative proteomics. *Journal of Biological Chemistry,* 281**,** 10024-10034.

BABA, T., ARA, T., HASEGAWA, M., TAKAI, Y., OKUMURA, Y., BABA, M., DATSENKO, K. A., TOMITA, M., WANNER, B. L. & MORI, H. 2006. Construction of *Escherichia coli* K-12 in-frame, single-gene knockout mutants: the Keio collection. *Molecular systems biology,* 2.

BACHMANN, J., BAUER, B., ZWICKER, K., LUDWIG, B. & ANDERKA, O. 2006. The Rieske protein from *Paracoccus denitrificans* is inserted into the cytoplasmic membrane by the twin-arginine translocase. *Federation of European Biochemical Societies Journal,* 273**,** 4817-4830.

BENSON, R., MEYER, R., ZARUBA, M. & MCKHANN, G. 1979. Cellular autofluorescence-is it due to flavins? *Journal of Histochemistry & Cytochemistry,* 27**,** 44-48.

BERKS, B. C. 1996. A common export pathway for proteins binding complex redox cofactors? *Molecular microbiology,* 22**,** 393-404.

BERTANI, G. 1951. Studies on lysogenesis I.: The mode of phage liberation by lysogenic *Escherichia coli*. *Journal of bacteriology,* 62**,** 293.

BLAUDECK, N., SPRENGER, G. A., FREUDL, R. & WIEGERT, T. 2001. Specificity of signal peptide recognition in Tat-dependent bacterial protein translocation. *Journal of bacteriology,* 183**,** 604-610.

BOLHUIS, A., MATHERS, J. E., THOMAS, J. D., BARRETT, C. M. & ROBINSON, C. 2001. TatB and TatC form a functional and structural unit of the twin-arginine translocase from *Escherichia coli*. *Journal of Biological Chemistry,* 276**,** 20213-20219.

BUCHRIESER, C., BROSCH, R., BACH, S., GUIYOULE, A. & CARNIEL, E. 1998. The high-pathogenicity island of *Yersinia pseudotuberculosis* can be inserted into any of the three chromosomal *asn* tRNA genes. *Molecular microbiology,* 30**,** 965-978.

CARRIÓ, M., GONZÁLEZ-MONTALBÁN, N., VERA, A., VILLAVERDE, A. & VENTURA, S. 2005. Amyloid-like properties of bacterial inclusion bodies. *Journal of molecular biology,* 347**,** 1025-1037.

CHEN, M., SAMUELSON, J. C., JIANG, F., MULLER, M., KUHN, A. & DALBEY, R. E. 2002. Direct interaction of YidC with the Sec-independent Pf3 coat protein during its membrane protein insertion. *Journal of Biological Chemistry,* 277**,** 7670-7675.

CHEREPANOV, P. P. & WACKERNAGEL, W. 1995. Gene disruption in *Escherichia coli*: Tc R and Km R cassettes with the option of Flp-catalyzed excision of the antibiotic-resistance determinant. *Gene,* 158**,** 9-14.

CHOPRA, I. & SHALES, S. 1980. Comparison of the polypeptide composition of *Escherichia coli* outer membranes prepared by two methods. *Journal of bacteriology,* 144**,** 425-427.

CLINE, K. & MORI, H. 2001. Thylakoid ΔpH-dependent precursor proteins bind to a cpTatC–Hcf106 complex before Tha4-dependent transport. *The Journal of cell biology,* 154**,** 719-730.

CONNOLLY, T., RAPIEJKO, P. J. & GILMORE, R. 1991. Requirement of GTP hydrolysis for dissociation of the signal recognition particle from its receptor. *Science (New York, NY),* 252**,** 1171-1173.

COX, M. M. 1983. The FLP protein of the yeast 2-microns plasmid: expression of a eukaryotic genetic recombination system in *Escherichia coli*. *Proceedings of the National Academy of Sciences,* 80**,** 4223-4227.

CRISTÓBAL, S., DE GIER, J. W., NIELSEN, H. & VON HEIJNE, G. 1999. Competition between Sec-and Tat-dependent protein translocation in *Escherichia coli*. *The European Molecular Biology Organization Journal,* 18**,** 2982-2990.

DALBEY, R. & WICKNER, W. 1985. Leader peptidase catalyzes the release of exported proteins from the outer surface of the *Escherichia coli* plasma membrane. *Journal of Biological Chemistry,* 260**,** 15925-15931.

DATSENKO, K. A. & WANNER, B. L. 2000. One-step inactivation of chromosomal genes in *Escherichia coli* K-12 using PCR products. *Proceedings of the National Academy of Sciences,* 97**,** 6640-6645.

DATTA, S., COSTANTINO, N. & COURT, D. L. 2006. A set of recombineering plasmids for Gram-negative bacteria. *Gene,* 379**,** 109-115.

DAVIS, W. 2013. *ApE - a plasmid editor* [Online]. Available: http://biologylabs.utah.edu/jorgensen/wayned/ape/.

DELISA, M. P., TULLMAN, D. & GEORGIOU, G. 2003. Folding quality control in the export of proteins by the bacterial twin-arginine translocation pathway. *Proceedings of the National Academy of Sciences,* 100**,** 6115-6120.

DILLINGHAM, M. S. & KOWALCZYKOWSKI, S. C. 2008. RecBCD enzyme and the repair of double-stranded DNA breaks. *Microbiology and Molecular Biology Reviews,* 72**,** 642-671.

DINH, T. & BERNHARDT, T. G. 2011. Using superfolder green fluorescent protein for periplasmic protein localization studies. *Journal of bacteriology,* 193**,** 4984-4987.

DONG, C., BEIS, K., NESPER, J., BRUNKAN-LAMONTAGNE, A. L., CLARKE, B. R., WHITFIELD, C. & NAISMITH, J. H. 2006. Wza the translocon for *E. coli* capsular polysaccharides defines a new class of membrane protein. *Nature,* 444**,** 226-229.

DREPPER, T., EGGERT, T., CIRCOLONE, F., HECK, A., KRAUß, U., GUTERL, J.-K., WENDORFF, M., LOSI, A., GÄRTNER, W. & JAEGER, K.-E. 2007. Reporter proteins for in vivo fluorescence without oxygen. *Nature biotechnology,* 25**,** 443-445.

DU PLESSIS, D. J., NOUWEN, N. & DRIESSEN, A. J. 2011. The sec translocase. *Biochimica et Biophysica Acta -Biomembranes,* 1808**,** 851-865.

DUONG, F. & WICKNER, W. 1997. The SecDFyajC domain of preprotein translocase controls preprotein movement by regulating SecA membrane cycling. *The European Molecular Biology Organization Journal,* 16**,** 4871-4879.

EGEA, P. F. & STROUD, R. M. 2010. Lateral opening of a translocon upon entry of protein suggests the mechanism of insertion into membranes. *Proceedings of the National Academy of Sciences,* 107**,** 17182-17187.

FILIP, C., FLETCHER, G., WULFF, J. L. & EARHART, C. 1973. Solubilization of the cytoplasmic membrane of *Escherichia coli* by the ionic detergent sodium-lauryl sarcosinate. *Journal of Bacteriology,* 115**,** 717-722.

FRÖBEL, J., ROSE, P., LAUSBERG, F., BLÜMMEL, A.-S., FREUDL, R. & MÜLLER, M. 2012. Transmembrane insertion of twin-arginine signal peptides is driven by TatC and regulated by TatB. *Nature communications,* 3**,** 1311.

GIBSON, D. G., YOUNG, L., CHUANG, R.-Y., VENTER, J. C., HUTCHISON, C. A. & SMITH, H. O. 2009. Enzymatic assembly of DNA molecules up to several hundred kilobases. *Nature methods,* 6**,** 343-345.

HARA, T., MATSUYAMA, S.-I. & TOKUDA, H. 2003. Mechanism underlying the inner membrane retention of *Escherichia coli* lipoproteins caused by Lol avoidance signals. *Journal of Biological Chemistry,* 278**,** 40408-40414.

HEIJNE, G. 1983. Patterns of amino acids near signal-sequence cleavage sites. *European journal of biochemistry,* 133**,** 17-21.

HELLMAN, J., LOISELLE, P. M., TEHAN, M. M., ALLAIRE, J. E., BOYLE, L. A., KURNICK, J. T., ANDREWS, D. M., KIM, K. S. & WARREN, H. S. 2000. Outer membrane protein A, peptidoglycan-associated lipoprotein, and murein lipoprotein are released by *Escherichia coli* bacteria into serum. *Infection and immunity,* 68**,** 2566-2572.

HICKS, M. G., DE LEEUW, E., PORCELLI, I., BUCHANAN, G., BERKS, B. C. & PALMER, T. 2003. The *Escherichia coli* twin-arginine translocase: conserved residues of TatA and TatB family components involved in protein transport. *Federation of European Biochemical Societies letters,* 539**,** 61-67.

HSU, P. D., LANDER, E. S. & ZHANG, F. 2014. Development and applications of CRISPR-Cas9 for genome engineering. *Cell,* 157**,** 1262-1278.

HUANG, B., BATES, M. & ZHUANG, X. 2009. Super resolution fluorescence microscopy. *Annual review of biochemistry,* 78**,** 993.

HUANG, Z., ZHANG, C., CHEN, S., YE, F. & XING, X.-H. 2013. Active inclusion bodies of acid phosphatase PhoC: aggregation induced by GFP fusion and activities modulated by linker flexibility. *Microbial Cell Factories,* 12**,** 25.

INVITROGEN. 2010. *Vectors for Dose-Dependent Expression of Recombinant Proteins Containing N- or C-Terminal 6×His Tags in E. coli* [Online]. Available: http://people.virginia.edu/~sf3bb/pbad_man.pdf.

KEFALA, G., KWIATKOWSKI, W., ESQUIVIES, L., MASLENNIKOV, I. & CHOE, S. 2007. Application of Mistic to improving the expression and membrane integration of histidine kinase receptors from *Escherichia coli*. *Journal of structural and functional genomics,* 8**,** 167-172.

KIEFER, D., HU, X., DALBEY, R. & KUHN, A. 1997. Negatively charged amino acid residues play an active role in orienting the Sec-independent Pf3 coat protein in the *Escherichia coli* inner membrane. *The European Molecular Biology Organization journal,* 16**,** 2197-2204.

KLENNER, C., YUAN, J., DALBEY, R. E. & KUHN, A. 2008. The Pf3 coat protein contacts TM1 and TM3 of YidC during membrane biogenesis. *Federation of European Biochemical societies letters,* 582**,** 3967-3972.

KMIEC, E. & HOLLOMAN, W. 1981. Beta protein of bacteriophage lambda promotes renaturation of DNA. *Journal of Biological Chemistry,* 256**,** 12636-12639.

KNIGHT, A. W. & BILLINTON, N. 2001. Distinguishing GFP from cellular autofluorescence. *Biophotonics International,* 8**,** 42-51.

KUMAMOTO, C. A. & BECKWITH, J. 1985. Evidence for specificity at an early step in protein export in *Escherichia coli*. *Journal of Bacteriology,* 163**,** 267-274.

KUMAZAKI, K., CHIBA, S., TAKEMOTO, M., FURUKAWA, A., NISHIYAMA, K.-I., SUGANO, Y., MORI, T., DOHMAE, N., HIRATA, K. & NAKADA-NAKURA, Y.

2014. Structural basis of Sec-independent membrane protein insertion by YidC. *Nature,* 509**,** 516-520.

LAMBERT, T. & THORN, K. *Fluorescent Protein Properies* [Online]. Available: http://nic.ucsf.edu/FPvisualization/.

LEAKE, M. C., GREENE, N. P., GODUN, R. M., GRANJON, T., BUCHANAN, G., CHEN, S., BERRY, R. M., PALMER, T. & BERKS, B. C. 2008. Variable stoichiometry of the TatA component of the twin-arginine protein transport system observed by in vivo single-molecule imaging. *Proceedings of the National Academy of Sciences,* 105**,** 15376-15381.

LENNOX, E. 1955. Transduction of linked genetic characters of the host by bacteriophage P1. *Virology,* 1**,** 190-206.

LITTLE, J. W. 1967. An exonuclease induced by bacteriophage λ II. Nature of the enzymatic reaction. *Journal of Biological Chemistry,* 242**,** 679-686.

MASUDA, K., MATSUYAMA, S.-I. & TOKUDA, H. 2002. Elucidation of the function of lipoprotein-sorting signals that determine membrane localization. *Proceedings of the National Academy of Sciences,* 99**,** 7390-7395.

MATSUYAMA, S. I., YOKOTA, N. & TOKUDA, H. 1997. A novel outer membrane lipoprotein, LolB (HemM), involved in the LolA (p20)-dependent localization of lipoproteins to the outer membrane of *Escherichia coli*. *The European Molecular Biology Organization journal,* 16**,** 6947-6955.

MEUSKENS, I. 2015. *Characterisation of a new overexpression strain for bacterial outer membrane proteins.* Eberhard Karls Universität Tübingen.

MICHE, B. 2010. *Chromosomal recombination with BL21* [Online]. Available: http://www.protocol-online.org/forums/topic/18731-chromosomal-recombination-with-bl21/.

MISRA, R., STIKELEATHER, R. & GABRIELE, R. 2015. In Vivo Roles of BamA, BamB and BamD in the Biogenesis of BamA, a Core Protein of the β-Barrel Assembly Machine of *Escherichia coli*. *Journal of molecular biology,* 427**,** 1061-1074.

MOORE, J. T., UPPAL, A., MALEY, F. & MALEY, G. 1993. Overcoming inclusion body formation in a high-level expression system. *Protein expression and purification,* 4**,** 160-163.

MUKHERJEE, A., WALKER, J., WEYANT, K. B. & SCHROEDER, C. M. 2013. Characterization of flavin-based fluorescent proteins: an emerging class of fluorescent reporters. *Public Library of Science one,* 8**,** e64753.

MURPHY, K. C. 1991. Lambda Gam protein inhibits the helicase and chi-stimulated recombination activities of *Escherichia coli* RecBCD enzyme. *Journal of bacteriology,* 173**,** 5808-5821.

NESTERENKO, M. V., TILLEY, M. & UPTON, S. J. 1994. A simple modification of Blum's silver stain method allows for 30 minite detection of proteins in polyacrylamide gels. *Journal of biochemical and biophysical methods,* 28**,** 239-242.

OSBORN, M., GANDER, J., PARISI, E. & CARSON, J. 1972. Mechanism of assembly of the outer membrane of *Salmonella typhimurium* isolation and characterization of cytoplasmic and outer membrane. *Journal of Biological Chemistry,* 247**,** 3962-3972.

OSBORN, M. & MUNSON, R. 1974. Separation of the inner (cytoplasmic) and outer membranes of Gram-negative bacteria. *Methods in enzymology,* 31**,** 642-653.

PALMER, T. & BERKS, B. C. 2012. The twin-arginine translocation (Tat) protein export pathway. *Nature Reviews Microbiology,* 10**,** 483-496.

PANAHANDEH, S., MAURER, C., MOSER, M., DELISA, M. P. & MÜLLER, M. 2008. Following the path of a twin-arginine precursor along the TatABC translocase of *Escherichia coli*. *Journal of Biological Chemistry,* 283**,** 33267-33275.

PAUTSCH, A. & SCHULZ, G. 1998. Structure of the outer membrane protein A transmembrane domain. *Nature Structural & Molecular Biology,* 5**,** 1013-1017.

PAUTSCH, A. & SCHULZ, G. E. 2000. High-resolution structure of the OmpA membrane domain. *Journal of molecular biology,* 298**,** 273-282.

PÉDELACQ, J.-D., CABANTOUS, S., TRAN, T., TERWILLIGER, T. C. & WALDO, G. S. 2006. Engineering and characterization of a superfolder green fluorescent protein. *Nature biotechnology,* 24**,** 79-88.

PISTON, D. W., CAMPBELL, R. E., DAY, R. N. & DAVIDSON, M. W. *Introduction to Fluorescent Proteins* [Online]. Available: http://zeiss-campus.magnet.fsu.edu/articles/probes/fpintroduction.html.

PUNGINELLI, C., MALDONADO, B., GRAHL, S., JACK, R., ALAMI, M., SCHRÖDER, J., BERKS, B. C. & PALMER, T. 2007. Cysteine scanning mutagenesis and topological mapping of the *Escherichia coli* twin-arginine translocase TatC Component. *Journal of bacteriology,* 189**,** 5482-5494.

RAPIEJKO, P. J. & GILMORE, R. 1994. Signal sequence recognition and targeting of ribosomes to the endoplasmic reticulum by the signal recognition particle do not require GTP. *Molecular biology of the cell,* 5**,** 887-897.

REUSCH, V. M. & BURGER, M. M. 1974. Distribution of marker enzymes between mesosomal and protoplast membranes. *Journal of Biological Chemistry,* 249**,** 5337-5345.

ROOSILD, T. P., GREENWALD, J., VEGA, M., CASTRONOVO, S., RIEK, R. & CHOE, S. 2005. NMR structure of Mistic, a membrane-integrating protein for membrane protein expression. *Science,* 307**,** 1317-1321.

ROOSILD, T. P., VEGA, M., CASTRONOVO, S. & CHOE, S. 2006. Characterization of the family of Mistic homologues. *BioMed central structural biology,* 6**,** 10.

ROSENBUSCH, J. P. 1974. Characterization of the major envelope protein from *Escherichia coli* regular arrangement on the peptidoglycan and unusual dodecyl sulfate binding. *Journal of Biological Chemistry,* 249**,** 8019-8029.

SANGER, F. & COULSON, A. R. 1975. A rapid method for determining sequences in DNA by primed synthesis with DNA polymerase. *Journal of molecular biology,* 94**,** 441-448.

SANKARAN, K. & WU, H. C. 1994. Lipid modification of bacterial prolipoprotein. Transfer of diacylglyceryl moiety from phosphatidylglycerol. *Journal of Biological Chemistry,* 269**,** 19701-19706.

SANTINI, C. L., IZE, B., CHANAL, A., MÜLLER, M., GIORDANO, G. & WU, L. F. 1998. A novel Sec-independent periplasmic protein translocation pathway in *Escherichia coli*. *The European Molecular Biology Organization Journal,* 17**,** 101-112.

SARGENT, F., BOGSCH, E. G., STANLEY, N. R., WEXLER, M., ROBINSON, C., BERKS, B. C. & PALMER, T. 1998. Overlapping functions of components of a bacterial Sec-independent protein export pathway. *The European Molecular Biology Organization Journal,* 17**,** 3640-3650.

SATO, K., MORI, H., YOSHIDA, M., TAGAYA, M. & MIZUSHIMA, S. 1997. In vitro analysis of the stop-transfer process during translocation across the cytoplasmic membrane of *Escherichia coli*. *Journal of Biological Chemistry,* 272**,** 20082-20087.

SCOTTI, P. A., URBANUS, M. L., BRUNNER, J., DE GIER, J. W. L., VON HEIJNE, G., VAN DER DOES, C., DRIESSEN, A. J., OUDEGA, B. & LUIRINK, J. 2000. YidC, the *Escherichia coli* homologue of mitochondrial Oxa1p, is a component of the Sec translocase. *The European Molecular Biology Organization journal,* 19**,** 542-549.

SEREK, J., BAUER-MANZ, G., STRUHALLA, G., VAN DEN BERG, L., KIEFER, D., DALBEY, R. & KUHN, A. 2004. *Escherichia coli* YidC is a membrane insertase for Sec-independent proteins. *The European Molecular Biology Organization journal,* 23**,** 294-301.

SHAN, S.-O. & WALTER, P. 2003. Induced nucleotide specificity in a GTPase. *Proceedings of the National Academy of Sciences,* 100**,** 4480-4485.

SHANER, N. C., CAMPBELL, R. E., STEINBACH, P. A., GIEPMANS, B. N., PALMER, A. E. & TSIEN, R. Y. 2004. Improved monomeric red, orange and yellow fluorescent proteins derived from *Discosoma* sp. red fluorescent protein. *Nature biotechnology,* 22**,** 1567-1572.

SHARAN, S. K., THOMASON, L. C., KUZNETSOV, S. G. & COURT, D. L. 2009. Recombineering: a homologous recombination-based method of genetic engineering. *Nature protocols,* 4**,** 206-223.

SIGMA-ALDRICH. *Product information Lysozyme from chicken egg white for Molecular Biology* [Online]. Available: https://www.sigmaaldrich.com/content/dam/sigma-aldrich/docs/Sigma/Datasheet/7/l7651dat.pdf.

SKLAR, J. G., WU, T., KAHNE, D. & SILHAVY, T. J. 2007. Defining the roles of the periplasmic chaperones SurA, Skp, and DegP in *Escherichia coli*. *Genes & development,* 21**,** 2473-2484.

SMIT, J., KAMIO, Y. & NIKAIDO, H. 1975. Outer membrane of *Salmonella typhimurium*: chemical analysis and freeze-fracture studies with lipopolysaccharide mutants. *Journal of Bacteriology,* 124**,** 942-958.

SONNTAG, I., SCHWARZ, H., HIROTA, Y. & HENNING, U. 1978. Cell envelope and shape of *Escherichia coli*: multiple mutants missing the outer membrane lipoprotein and other major outer membrane proteins. *Journal of bacteriology,* 136**,** 280-285.

STEFANIE, S., FRIEDHELM, P., KIERAN, D., QIANG, C. Z., SAHEED, I. & MECHTHILD, P. 2010. Mutational and bioinformatic analysis of haloarchaeal lipobox-containing proteins. *Archaea,* 2010.

STUDIER, F. W. 2005. Protein production by auto-induction in high-density shaking cultures. *Protein expression and purification,* 41**,** 207-234.

SUBRINI, O. & BETTON, J.-M. 2009. Assemblies of DegP underlie its dual chaperone and protease function. *Federation of European Microbiological Societies microbiology letters,* 296**,** 143-148.

TARRY, M. J., SCHÄFER, E., CHEN, S., BUCHANAN, G., GREENE, N. P., LEA, S. M., PALMER, T., SAIBIL, H. R. & BERKS, B. C. 2009. Structural analysis of substrate binding by the TatBC component of the twin-arginine protein transport system. *Proceedings of the National Academy of Sciences,* 106**,** 13284-13289.

TERADA, M., KURODA, T., MATSUYAMA, S.-I. & TOKUDA, H. 2001. Lipoprotein sorting signals evaluated as the LolA-dependent release of lipoproteins from the cytoplasmic membrane of *Escherichia coli*. *Journal of Biological Chemistry,* 276**,** 47690-47694.

THEIN, M., SAUER, G., PARAMASIVAM, N., GRIN, I. & LINKE, D. 2010. Efficient subfractionation of Gram-negative bacteria for proteomics studies. *Journal of proteome research,* 9**,** 6135-6147.

UEHARA, T., PARZYCH, K. R., DINH, T. & BERNHARDT, T. G. 2010. Daughter cell separation is controlled by cytokinetic ring-activated cell wall hydrolysis. *The European Molecular Biology Organization journal,* 29**,** 1412-1422.

VAN DEN BERG, B., CLEMONS, W. M., COLLINSON, I., MODIS, Y., HARTMANN, E., HARRISON, S. C. & RAPOPORT, T. A. 2004. X-ray structure of a protein-conducting channel. *Nature,* 427**,** 36-44.

VON HEIJNE, G. 1989. The structure of signal peptides from bacterial lipoproteins. *Protein engineering,* 2**,** 531-534.

WALTER, P. & BLOBEL, G. 1981. Translocation of proteins across the endoplasmic reticulum. II. Signal recognition protein (SRP) mediates the selective binding to microsomal membranes of in-vitro-assembled polysomes synthesizing secretory protein. *The Journal of cell biology,* 91**,** 551-556.

WALTON, T. A., SANDOVAL, C. M., FOWLER, C. A., PARDI, A. & SOUSA, M. C. 2009. The cavity-chaperone Skp protects its substrate from aggregation but allows independent folding of substrate domains. *Proceedings of the National Academy of Sciences,* 106**,** 1772-1777.

WU, T., MALINVERNI, J., RUIZ, N., KIM, S., SILHAVY, T. J. & KAHNE, D. 2005. Identification of a multicomponent complex required for outer membrane biogenesis in *Escherichia coli*. *Cell,* 121**,** 235-245.

YAKUSHI, T., MASUDA, K., NARITA, S.-I., MATSUYAMA, S.-I. & TOKUDA, H. 2000. A new ABC transporter mediating the detachment of lipid-modified proteins from membranes. *Nature cell biology,* 2**,** 212-218.

YAMAGUCHI, K., YU, F. & INOUYE, M. 1988. A single amino acid determinant of the membrane localization of lipoproteins in *E. coli*. *Cell,* 53**,** 423-432.

YU, W. & GÖTZ, F. 2012. Cell wall antibiotics provoke accumulation of anchored mCherry in the cross wall of *Staphylococcus aureus*. *Public Library of Science one,* 7**,** e30076.

ZIMMER, J., NAM, Y. & RAPOPORT, T. A. 2008. Structure of a complex of the ATPase SecA and the protein-translocation channel. *Nature,* 455**,** 936-943.

Appendix 1 Abbreviations

The abbreviations used throughout the thesis, ordered alphabetically.

Abbreviation	Full name
ΔABCF	Δ *LamB, OmpA, OmpC, OmpF*
A	Alanine
ATP	Adenosine 5’ -triphosphate
B. subtilis	*Bacillus subtilis*
BAM	β – barrel assembly machinery
BSA	Bovine Serum Albumin
C	Cysteine
D	Aspartatic acid
dsDNA	Double stranded DNA
E. coli	*Escherichia coli*
EcFbFP	*Escherichia coli* Flavin mononucleotide binding Fluorescent Protein
FbFP	Flavin mononucleotide binding fluorescent protein
FMN	Flavin mononucleotide
FRT	Flp recombination target
G	Glycine
GFOR	Glucose-fructose oxidoreductase
GFP	Green Fluorescent Protein
GSGS	Glycine-serine-glycine-serine
GTP	Guanosine 5’-triphosphate

Appendix 1

IM	Inner membrane
IPTG	Isopropyl β-D-1-thiogalactopyranoside
kDa	Kilo Daltons
L	Leucine
LB	Lysogeny broth
Lep	Leader peptidase
Lol	Localization of lipoproteins
LPS	Lipopolysaccharide
NADH	β-Nicotineamide Adenine Dinucleotide
NEB	New England BioLabs®
OD_{600}	Optical density
OM	Outer membrane
OmpA	Outer membrane protein A
PCR	Polymerase Chain Reaction
pf3	Phage pf3 major coat protein
S	Serine
SD	Standard deviations
SDS-PAGE	Sodium dodecyl sulphate polyacrylamide gel electrophoresis
Sec	General Secretion
sfGFP	Superfolder green fluorescent protein
SOEing	Splicing by Overlap Extension
SRP	Signal recognition particle
ssDNA	Single stranded DNA

Tat	Twin Arginine
TMS(s)	Transmembrane segment(s)

Appendix 2 Primer sequences

All primers were designed manually and manufactured by LifeTechnologies™ unless otherwise indicated. All primers are displayed in the form of 5' – 3'.

Cloning of fusion genes into pACYCDuet-1

Name	Sequence
OmpA Fwd	ATAAGGAGATATACCATGAAAAAGACAGCTATCGCGATT
GSGS ompA rev	GCTACCGCTGCCACCGAAACGGTAGGAAACACCCAG
OmpA-mCherry Fwd	GGTGGCAGCGGTAGCGTGAGCAAGGGCGAGGA
mCherry Rev	TGTTCGACTTAAGCACTACTTGTACAGCTCGTCC
Tat-lipo Fwd	AGGAGATATACCATGAACAATAACGATCTCTTTCAG
Tat-lipo Rev	ATCGCAGCCCGCCAGCGCTTGCGCCGCAGTC
Tat-EcFbFP Fwd	CTGGCGGGCTGCGATGCGTCGTTCCAGTCGTTCGG
EcFbFP Rev	TGTTCGACTTAAGCATTACTCGAGCAGCTTTTCATATTC
Pf3 Fwd1	AGGAGATATACCATGCAATCCGTGATTACTGATGTGACAGGCCAACTGACAGCGGTGCAA
Pf3 Rev1	ACAGCGGCCAGAACAATAATAGCACCACCAATGGTAGTGATATCAGCTTGCACCGCTGTCAGTT
Pf3 Fwd2	ATTGTTCTGGCCGCTGTTGTGCTGGGTATTCGCTGGATCAAAGCGCAATTCTTT
EcFbFP-pf3 Rev2	CGACTGGAACGACGCACCAGAGCCGCTAAAGAATTGCGCTTTGATCCAG
EcFbFP Fwd	GCGTCGTTCCAGTCGTTCGG
EcFbFP Rev	TGTTCGACTTAAGCATTACTCGAGCAGCTTTTCATATTC
Mistic Fwd	AGGAGATATACCATGTTTTGTACATTTTTTGAAAAACATCAC
Mistic Rev	GCTACCGCTGCCTTCTTTTTCTCCTTCTTCAGATACTGA
Mistic-EcFbFP Fwd	GAAGGCAGCGGTAGCGCGTCGTCCCAGTCGTTCGG
Mistic-sfGFP Fwd	GAAGGCAGCGGTAGCGCATCAAAAGGTGAAGAATTATTTA
sfGFP Rev	TGTTCGACTTAAGCATTATTTATATAATTCATCCATACCATGTG

Appendix 2

GSGS pf3 Rev2	GCTACCGCTGCCAAAGAATTGCGCTTTGATCCAG
pf3-sfGFPF Fwd	TTTGGCAGCGGTAGCGCATCAAAAGGTGAAGAATTATTTA
pACYCDuetMCS1 Fwd	TTGTACACGGCCGCATAA
pACYCDuetMCS1 Rev	GATTATGCGGCCGTGTACAA
OmpA MCS2 Fwd	GAAGGAGATATACATATGAAAAAGACAGCTATCGCGATTG
mCherry MCS2 Rev	CTCGAGGGTACCGACGTCCTACTTGTACAGCTCGTCCA
pACYCDuetMCS2 Fwd	TAATTAACCTAGGCTGCTGCCAC
pACYCDuetMCS2 Rev	CATATGTATATCTCCTTCTTATACTTA

λ red recombination

Scar-ompA Fwd	GTTGGAGATATTCATGGCGTATTTTGGATGATAACGAGGCGCAAAAAATGAAAAAGAC AGCTATCGCGATTG
Scar- mCherry Rev	GCAGCGGGGTTTTTCTACCAGACGAGAACTTAAGCCTGCGGCTGAGTTACCTACTTGTAC AGCTCGTCC
Asnt-con1 Fwd	TCAACAACGATTCCTCTGTAGTTCAGTCGGTAGAACGGCGGACTGTTAATTTGACGGCTAG CTCAGTCC
Con1-ompA Rev	GCGATAGCTGTCTTTTTCATGGTTAATTCCTCCTGTTAGCCCAAAAAACGGGTATGGCTAGC ACTGTACCTAGGA
ompA Fwd	ATGAAA AAGACAGCTATCGCG
mCherry Rev	CTACTTGTACAGCTCGTCCA
mCherry-term Fwd	TGGACGAGCTGTACAAGTAGCTAGCATAACCCCTTGGGG
term-Km Rev	TCCCCGGAATATGCATGCAT CAAAAAACCCCTCAAGACCC
Km Fwd	ATGCATGCATATTCCGGGGATCCGTCGA
Km-Asnt Rev	CTTTTCAGGAATTTGGCTCCTCTGACTGGACTCGAACCAGTGACATACGGTGTAGGCTGGAGC TGCTTC

Sequencing of fusion genes in pACYCDuet-1

pACYCDuet-1 Fwd*	GGATCTCGACGCTCTCCCT
pACYCDuet-1 Rev*	GCTAGTTATTGCTCAGCGG

*The sequencing primers for pACYCDuet-1 were manufactured by Sigma Aldrich®.

Sequencing of fusion genes in the *E. coli* BL21 Gold (DE3) genome

OmpA scar seq Fwd	GGTGAAGGATTTAACCGTGTTAT
OmpA scar seq Rev	TGACGAAAGTCAGTTCAATTTACT
Asnt seq Fwd	ATA GAA ACG GCA AAC AGT TGG
Asnt seq Rev	C AGG TGA TGG AAA GCA GTG

Appendix 3 λ Red Recombination insertion sites

Insertion sites in the *E. coli* BL21 Gold (DE3) genome used in λ red recombination.

Insertion site	**Sequence**
OmpA scar fwd	5’-GTTGGAGATATTCATGGCGTATTTTGGATGATAACGAGGCGCAAAAAATG-3’
mCherry scar rev	5’-GCAGCGGGGTTTTTCTACCAGACGAGAACTTAAGCCTGCGGCTGAGTTAC-3’
AttB fwd	5’-CAGTTGATTCAAAATCAACCGTAGAAATACGTGCCGGTTCGAGTCCGGCC-3’
AttB rev	5’-TTCGGCACCAAAAGTATGTAAATAGACCTCAACTGAGGTCTTTTTTTATG-3’
AsnU fwd	5’-TCAACAACGATTCCTCTGTAGTTCAGTCGGTAGAACGGCGGACTGTTAAT-3’
AsnU rev	5’-CCGTATGTCACTGGTTCGAGTCCAGTCAGAGGAGCCAAATTCCTGAAAAG-3’

Appendix 4 Buffers, solutions and chemicals

Buffers, solutions and chemicals used in this project, cited in Materials and methods, section 2.

Agarose gels and corresponding buffers

Table 1 shows the components of 10xTBE buffer used to make agarose gels, DNA stain and DNA loading buffer.

Table 1: Components in 10 x TBE buffer, 1 % agarose gels, DNA gel stain, and 6 x DNA sample buffer.

Solution	**Component**	**Company**
10xTBE	108 g Tris	Angus
	55 g Boric acid	Sigma
	7 g EDTA	AppliChem
	Water to 1 l	
Agarose	SeaKem®LE Agarose	LONZA
SYBR® Safe DNA gel stain		Invitrogen™
6x DNA loading buffer	3,5 ml 100% glycerol	VWR AnalaR Normapur
	35 µl 3 M Tris-HCl, pH 8,0	Angus
	20 µl 0,5 M EDTA, pH 8,0	AppliChem
	25 mg bromphenol blue Sodium salt	Sigma
	H_2O to 10 ml	

Lysogeny Broth and LB agar plates

Table 2 displays the components of LB broth used in the project. The broth with 5 g NaCl was used for growth of BL21 (DE3) ΔABCF. Table 3 displays the components in the LB agar plates used in the project.

Appendix 4

Table 2: Components of lysogeny broth. The low salt LB medium for BL21 (DE3) ΔABCF contains 5 g NaCl.

Media	**Components**	**Company**
LB	5 g/10 g NaCl	AnalaR
	10 g Tryptone	Fluka
	5 g yeast extract	VWR

Table 3: Components of LB agar for plates.

	Components	**Company**
LB agar	25 g LB broth	BD
	10 g Bactopor agar	BD
	dd H_2O to 1 l	

Autoinduction media

Table 4 contains the components of the autoinduction media ZYP-5052.

Table 4: Autoinduction media used for induction of expression from the *lac* promoter in *E. coli* BL21 Gold (DE3)

Media	**Components**	**Company**
ZY	10 g N-Z-amine AS (or tryptic digest of casein)	Fluka
	5 g yeast extract	VWR chemicals
	925 ml H2O	
50x5052	25g glycerol	VWR chemicals
	2.5 g D(+)-glucose-monohydrate	Merck
	10g lactose-monohydrate	VWR chemicals
	73 ml H2O	

20xNPS	66 g $(NH_4)_2SO_4$	Merck
	136 g KH_2PO_4	Merck
	142 g Na_2HPO_4	VWR chemicals
ZYP-5052	930 ml ZY medium	
	1 ml 1M MgSO4	Merck
	50 ml 20xNPS	
	20 ml 50x5052	

Buffers and solution in membrane separation

Table 5 displays the buffers and solutions used in the two membrane separation techniques in this project.

Table 5: Buffers and solution used in the membrane separation techniques.

Buffer/solution	**Component**	**Company**
HEPES buffer 10mM MgSO4, pH 7,4	HEPES	Sigma
	MgSO4	MERCK
2 % N-lauroylsarcosine	N-lauroylsarcosine sodium salt	Sigma
Sucrose solutions for creating a gradient for separation	Sucrose	Sigma
	Tris	Angus
	EDTA	AppliChem
Sucrose solution for dissolving membrane pellet before loading on gradient	Sucrose	Sigma
	Tris	Angus
	EDTA	AppliChem
	DTT	

Appendix 4

SDS-PAGE gels, buffers, and stains

Table 6 displays the components required to make a stack of four 15 % polyacrylamide gels, while Table 7 shows the components in the 4X SDS loading buffer and the 10X SDS running buffer. Tables 8 and 9 display the component used for Coomassi staining and destaining, and silver staining, respectively.

Table 6: Components to make a stack of four 15 % polyacrylamide gels.

Gel	**Components**	**Company**
Stacking gel	5.9 ml Water	
	2.5 ml 1 M Tris, pH 6,8	Angus
	1.4 ml 30 % Acrylamide	AppliChem
	100 µl 10 % SDS	AppliChem
	10 µl TEMED	GE Health care
	100 µl 10 % APS	Sigma
Separation gel	6.9 ml water	
	7.5 ml 1.5 M Tris, pH 8.8	Angus
	15 ml 30 % Acrylamide	AppliChem
	300 µl 10 % SDS	AppliChem
	30 µl TEMED	GE Health care
	300 µl 10 % APS	Sigma

Table 7: Components in 4 x SDS-PAGE sample buffer and 1 x SDS-PAGE running buffer.

Buffer	**Components**	**Company**
4 X SDS-PAGE sample buffer	8 % SDS	AppliChem
	0.1 % bromphenol blue sodium salt	Sigma
	200 mM Tris pH 6.8	Angus

	40 % glycerol	VWR chemicals
	1 mM EDTA	AppliChem
	ddH_2O	
10 X SDS-PAGE running buffer	30 g Tris	Angus
	144 g glycine	VWR chemicals
	10 g SDS	AppliChem
	Water to 1 l	

Table 8: Components in Coomassie Brilliant Blue R250 staining solution and destaining solution.

Solution	**Component**	**Company**
Coomassi Brilliant Blue staining solution	1 g Brilliant Blue R250	Sigma
	10 % acetic acid	Sigma
	50 % ethanol	Arcus
	ddH2O to 1 l	
Destain solution	30 % ethanol	Arcus
	10 % acetic acid	Sigma
	ddH2O to 1 l	

Table 9: Components in the silver staining technique.

Step	**Solution**	**Company**
Fixation	60 ml 50 % acetone	VWR chemicals
	1,5 ml 50 % TCA	Sigma

	25 µl 37 % HCHO	Sigma
Rinse	60 ml ddH_2O	
Wash	60 ml ddH_2O	
Rinse	60 ml ddH_2O	
Pretreat	60 ml 50 % acetone	VWR chemicals
Pretreat	100 µl 10 % $Na_2S_2O_3*5H_2O$ in 60 ml ddH_2O	Fluka
Rinse	60 ml ddH_2O	
Impregnate	0.8 ml 20 % $AgNO_3$	AppliChem
	0.6 ml 37 % HCHO	Sigma
	60 ml ddH_2O	
Rinse	60 ml ddH_2O	
Develop	1.2 g Na_2CO_3	Merck
	25 µl 37 % HCHO	Sigma
	25 µl 10 % $Na_2S_2O_3*5H_2O$	Fluka
	60 ml ddH_2O	
Stop	1 % glacial acetic acid in ddH_2O	Sigma
Rinse	60 ml ddH_2O	

Western blot

Table 10 shows the components required to make Western transfer buffer and 1X PBST used in Western blotting.

Table 10: Chemicals and solutions used in western blotting.

Solution	**Component**	**Company**
Western transfer buffer	25 mM Tris	Angus

	150 mM glycine	VWR Chemicals
	10 % isopropanol	Sigma-Aldrich
1 x PBST	8 g NaCl	VWR Chemicals
	0.2 g KCl	Merck
	1.44 g Na_2HPO_4	VWR Chemicals
	0.24 g KH_2PO_4	Merck
	2 ml Tween-20	Sigma
Bovine Serum Albumin		VWR Chemicals

NADH oxidase enzymatic assay

Table 11 displays the buffers and chemicals used in the NADH oxidase assay utilized in this project.

Table 11: Solutions used in the NADH oxidase assay.

Solution	**Component**	**Company**
250 mM potassium phosphate buffer pH 7.0	Potassium Phosphate	Merck
1 Mm Flavin Adenine Dinucleotide	Flavin Adenine Dinucleotide	Sigma
2 mM β – nicotineamide Adenine Dinucleotide	β – nicotineamide Adenine Dinucleotide	Sigma
30 mM potassium phosphate buffer with 0.1 % Bovine Serum Albumin, pH 7.5	Potassium phosphate	Merck
	Bovine Serum Albumin	VWR chemicals